110

SPIRALING FLOW THROUGH AN ECCENTRIC ANNULUS

A THESIS SUBMITTED TO
THE GRADUATE SCHOOL OF NATURAL AND APPLIED SCIENCES
OF
THE MIDDLE EAST TECHNICAL UNIVERSITY

BY

TEVFİK KUTAY ÇELEBİOĞLU

119280

IN PARTIAL FULFILLMENT OF THE REQUIREMENTS FOR THE DEGREE OF
MASTER OF SCIENCE
IN
THE DEPARTMENT OF CIVIL ENGINEERING

119280

AUGUST 2002

Approval of the Graduate School of Natural and Applied Sciences

Prof. Dr. Tayfur ÖZTÜRK
Director

I certify that this thesis satisfies all the requirements as a thesis for the degree of Master of Science.

Prof. Dr. Mustafa TOKYAY
Head of Department

This is to certify that we have read this thesis and that in our opinion it is fully adequate, in scope and quality, as a thesis for the degree of Master of Science.

Prof Dr. Turgut TOKDEMİR
Co-Supervisor

Prof. Dr. Metin GER
Supervisor

Examining Committee Members

Prof. Dr. Kahraman ALBAYRAK (Mechanical Eng.)

Prof. Dr. Metin GER

Assoc. Prof. Dr. İsmail AYDIN

Assist. Prof. Dr. Zafer BOZKUŞ

Dr. Şahnaz TİĞREK

ABSTRACT

SPIRALING FLOW THROUGH AN ECCENTRIC ANNULUS

Çelebioğlu, Tevfik Kutay

M.S., Department of Civil Engineering

Supervisor: Prof. Dr. A. Metin Ger

Co-Supervisor: Prof. Dr. Turgut Tokdemir

August 2002, 93 Pages

In this study, a new, recently popular numerical method is applied to a fluid mechanics problem. The basics of the method, which is the Generalized Finite Difference Method (GFD) or Meshless Method, are given.

The method is applied to a well-known cavity problem to validate the formulation of the method. The capability of the method is tested on the flow through an eccentric annulus. Vorticity–Stream function formulation is used to handle the

flow phenomena. Case studies for different Reynolds numbers and different eccentricities are performed. The velocity vector plots and streamlines are drawn for each case. The results for concentric cases are compared with the theoretical solution of the problem.

Keywords: Eccentric cylinders, generalized finite difference, meshless method.

ÖZ

EKSANTRİK SİLİNDİRLER ARASINDAKİ DÖNEN AKIM

Çelebioğlu, Tevfik Kutay

Yüksek Lisans, İnşaat Mühendisliği Bölümü

Tez Yöneticisi: Prof. Dr. A. Metin Ger

Ortak Tez Yöneticisi: Prof. Dr. Turgut Tokdemir

Ağustos 2002, 93 Sayfa

Bu tezde, yeni ve son zamanlarda çok kullanılan bir sayısal çözümleme metodu akışkanlar mekaniği problemlerine uygulanmıştır. Genelleştirilmiş Sonlu Fark Metodu ya da Izgarasız Metot adı verilen yöntemin temelleri verilmiştir.

Yöntemi teyit etmek için, yöntem kavite problemine uygulanmıştır. Yöntemin özellikleri, eksenleri çakışık olmayan silindirler arasındaki akım için test edilmiştir. Akışı incelemek için çevrinti–akış fonksiyonu formülasyonu

kullanılmıştır. Farklı Reynolds sayıları ve farklı eksantriklikler için örnek çalışmalar yapılmıştır. Her örnek için, hız dağılımları ve akış çizgileri programdan sonuç olarak elde edilmiştir. Eksenleri çakışık olan silindirler arasındaki akışın sayısal sonuçları teorik çözümle karşılaştırılmıştır.

Anahtar kelimeler: Eksantrik silindirler, genelleştirilmiş sonlu fark metodu, ızgarasız metot.

T.C. YÜKSEKÖĞRETİM KURULU
DOKÜMANTASYON MERKEZİ

To My Family

ACKNOWLEDGMENTS

I would like to express my gratitude to my thesis supervisor Prof. Dr. Metin Ger and co-supervisor Prof. Dr. Turgut Tokdemir for their support, guidance and suggestions throughout the analysis and completion of this thesis.

I would like to thank to my friend Burak Sapaz for his help, technical support, comments and friendship. My thanks also go to Volkan Yargıcı and Ö. Uğraş Baran for their friendship and comments at certain stages of the thesis.

I owe special thanks to my parents Nejat and Dilek Çelebioğlu for preparing a perfect studying environment for me, continuous support throughout the thesis and for their love. I would also like to thank to my little sister Sena Çelebioğlu for her endless love.

Finally, I would like to thank to my wife Selin Aradağ Çelebioğlu not only for her love but also for her invaluable support throughout this thesis. I would not be able to finish this thesis without her help.

T.C. YÜKSEKÖĞRETİM KURULU
DOKÜMANTASYON MERKEZİ

TABLE OF CONTENTS

T.C. YÜKSEKÖĞRETİM KURULU
DOKÜMANTASYON MERKEZİ

LIST OF TABLES

TABLE

T.C. YÜKSEKÖĞRETİM KURULU
DOKÜMANTASYON MERKEZİ

LIST OF FIGURES

FIGURE

NOMENCLATURE

c_r: Courant number.

d: The distance between two nodes.

f: Any arbitrary function.

h: The difference of x coordinates of two nodes.

i: Integers ranging from 1 to n.

k: The difference of y coordinates of two nodes.

n: Number of nodes in the system.

r: The first coordinate of the cylindrical coordinate system

t: time.

u: x-component of the velocity vector.

v: y-component of the velocity vector.

x: First coordinate of a node for a global x-y coordinate system.

y: Second coordinate of a node for a global x-y coordinate system.

w: A weight function for minimization.

B: A norm that is to be minimized.

Df: A vector containing derivatives.

Ecc: Eccentricity of cylinders.

F: A vector containing combination of function values.

P: Pressure.

T.C. YÜKSEKÖĞRETİM KURULU
DOKÜMANTASYON MERKEZİ

Re: Reynolds number.

α: First derivative of any function f with respect to x.

β: First derivative of any function f with respect to y.

γ: Second derivative of any function f with respect to x.

δ: Second derivative of any function f with respect to y.

ε: Derivative of any function f with respect to x and y respectively.

ρ: Density of fluid.

υ: Kinematic viscosity.

μ: Dynamic viscosity.

ς: Vorticity.

ω: Angular velocity.

Φ: A function given in equation 3.9.

ψ: Stream function.

θ: The second coordinate of the cylindrical coordinate system.

CHAPTER 1

FLOW THROUGH AN ECCENTRIC ANNULUS

1.1 General

Flows in annular passages are important in drilling wells where fluid passes between the drill shaft and the well casing. There are also several other engineering applications like journal bearings, biological separation devices, rotating machinery and heat exchangers. Knowledge of the fluid motion in such examples is needed at the design stage to predict hydrodynamic behavior and hence torque and heat transfer characteristics in relation to the transport properties of the working fluid.

Drilling muds are used to drill oil and gas wells. During drilling operations these liquid muds are pumped from a surface mud tank through the drill pipe, several kilometers in length, through nozzles in the rotating drill bit, and back to the mud tank through the annular space between the well bore wall and the drill pipe. Since the annual cost of the drilling operations runs into billions of dollars, it comes as no surprise that; the oil industry has invested heavily in research into the flow of drilling mud. Calculation of the flow down to drill pipe is relatively

straightforward whereas the flow through the drill bit nozzles and in the region of the workface is turbulent and extremely complex. From a practical point of view interest focuses on the variation in mud pressure within the well bore and, to some degree, the hydraulic torque (i.e. the torque exerted on the rotating drill string by the surrounding mud). The underlying challenge to fluid dynamicists has been to calculate the flow field within the drillstring-wellbore annulus, a situation usually idealized as that of steady, isothermal, fully developed laminar flow of a shear-thinning liquid (modeled as a generalized Newtonian fluid) through an annulus consisting of an outer cylinder and an inner cylinder which may be offset and rotating.

Although the drilling of oil wells is the most important, there are numerous other applications, which require a detailed understanding of the annular flow of non-Newtonian liquids. Such applications include oil-well completion operations and are also found in industries dealing with industrial waste, with slurries and suspensions such as processed foodstuffs, synthetic fibers and even blood, and with the extrusion of molten plastics and polymer solutions.

In recent years, heat transfer problems in non-circular ducts have become important. Tube misalignment in a close-packed tubular heat exchanger often causes serious damage to heat transfer equipment. In the case of nuclear reactors, in particular it has been pointed out that misalignment of a fuel rod caused by

thermal stress finally leads to the local meltdown of the fuel rod. The flow in an annulus is useful as a model for longitudinal flow in a tube bundle.

In many branches of nuclear research, the exchange of heat inside the reactor of the heavy water demands, beside a specific heat energy, an exact check on the limited values of the decrease in pressure inside the reactor. It also demands exact information about the volume of the wanted heavy water, which must be as little as possible. With regard to the last demand, special technical constructions of the heat exchanger apparatus should be needed. Such apparatus may be composed of arranged concentric of eccentric cylinders, so that the inner space between them is very small to allow flow of little heavy water.

An important problem associated with the design and application of certain types of journal bearings and pressure-reducing bushings as employed in turbomachinery in the form of wearing rings, labyrinth seals, balancing drums, and pressure-breakdown devices, involves the determination of fluid flow through annuli of fine clearance, i.e., one or more spaces bounded axially by two cylindrical bodies of slightly different diameters nesting with varying degrees of eccentricity. A search of the published information reveals that many factors have an effect on the magnitude of the flow through these passages, the most significant ones being clearance, length, rotation, eccentricity, surface condition, and fluid properties.

The interest in eccentric annulus arises because of the misalignment of the tubes, deformations due to large pressure or thermal forces and vibrations caused by the high turbulence.

Knowledge of the hydrodynamic behavior in relation to the transport properties of working fluid is needed. Both the axial stability and the rotational stability of the flow should be maintained.

Various experimental and numerical studies have been made on this subject standing on the Taylor's analysis of the stability of circular Couette flow and later extended to the axial flow.

1.2 Description of the Problem

If the annulus is infinitely long and the only cause for the flow is the rotation of the inner cylinder (i.e. no pressure gradient in the axial direction) then the flow is assumed to be two-dimensional. The geometry of the eccentric annulus is given in Figure 1.1.

T.C. YÜKSEKÖĞRETİM KURULU
DOKÜMANTASYON MERKEZİ

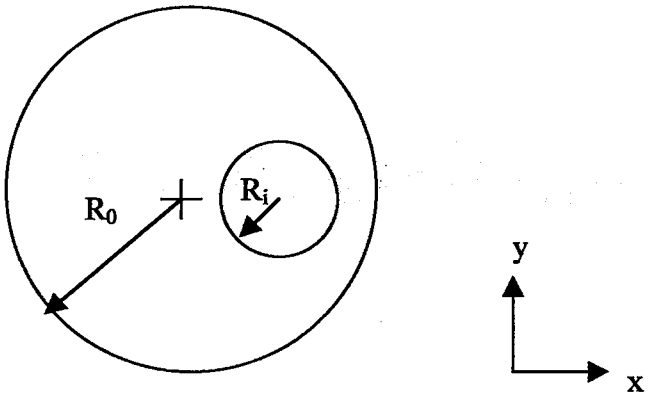

Figure 1.1 The geometry of the eccentric annulus

Where the R_i and the R_o represent the inner and the outer cylinders radius, respectively. And Ecc is the eccentricity between the two cylinders. The inner cylinder is rotating with an angular speed of "ω" in counter clockwise direction and the gravitational force is in negative z-direction which passes through central axis

For the mathematical treatment, the flow is assumed to be:

- Incompressible
- Laminar (no turbulence modeling is done)
- No heat convection exists.

Then the governing equations can be written from the Navier-Stokes equations in x and y-directions respectively as:

$$\frac{\partial u}{\partial t}+u\frac{\partial u}{\partial x}+v\frac{\partial u}{\partial y}=-\frac{1}{\rho}\frac{\partial p}{\partial x}+\upsilon\left(\frac{\partial^2 u}{\partial x^2}+\frac{\partial^2 u}{\partial y^2}\right) \tag{1.1}$$

$$\frac{\partial v}{\partial t}+u\frac{\partial v}{\partial x}+v\frac{\partial v}{\partial y}=-\frac{1}{\rho}\frac{\partial p}{\partial y}+\upsilon\left(\frac{\partial^2 v}{\partial x^2}+\frac{\partial^2 v}{\partial y^2}\right) \tag{1.2}$$

And the continuity equation:

$$\frac{\partial u}{\partial x}+\frac{\partial v}{\partial y}=0 \tag{1.3}$$

For the steady-state solution of the Navier-Stokes equations, the time derivative drops out. Analytical solutions of these equations are unattainable and a numerical method for solving partial differential equations should be applied.

In a number of experimental researches it was found that Taylor's vortices are seen on the flow pattern depending on the Reynolds number, eccentricity, and diameter ratio.

1.3 The Aim and Scope of This Study

The thesis employs a recently developed numerical solution technique applied to the flow through an eccentric annulus. The numerical method used is the

generalized finite difference method, also called the meshless method. A computer program has been developed to find the solution of the flow between two eccentric cylinders, using the generalized finite difference method.

CHAPTER 2

LITERATURE SURVEY

2.1 General

The previous work in literature related to the spiraling flow through an eccentric annulus, numerical methods relevant to the solution, papers about the boundary conditions, methods used for the numerical solution of flow through an annulus other than generalized finite difference method, which is used in this study, are summarized in this chapter. Literatures relevant to these topics are given under separate headings.

2.2 Literature related to the flow through an eccentric annulus

The study by Dai, Dong and Szeri (1992) is about the flow between eccentric rotating cylinders, bifurcation and stability [6]. The effect of cylinder eccentricity on Couette-Taylor transition is investigated in the study for the flow between infinite rotating cylinders. The method of analysis is Fourier expansion of the conservation equations in the axial direction, followed by projection onto a polynomial subspace. The computational scheme of the study permits high values

of the eccentricity ratio, it also makes it possible to move far from the critical point into the supercritical (in terms of a certain Taylor's number) Reynolds number regime. The first bifurcation from Couette flow is found to be supercritical, while supercritical flow is shown to consist of regions of plane motion with recirculation, separating toroidal vortex regions. The domain of recirculating flow is asymmetric with respect to the line of centers, and on increasing the supercritical Reynolds number its axial dimension decreases while its radial dimension, in the plane separating the vortex cells, increases.

An analysis of fully developed turbulent flow in an eccentric annulus is presented by Usui and Tsuruta (1980) [7]. An integral transformation technique (Kirchhoff transformation) is applied to eccentric annuli in a wide range of eccentricity and radius ratio. Velocity distributions, wall shear stress distributions and friction factors are calculated and compared with the literature. Although the analysis can not predict the secondary flow in an eccentric annulus, the calculated results show good agreement with the experimental results in the literature.

Several experiments on turbulent-flow phenomena in eccentric annular ducts are performed by Jonsson and Sparrow (1966) [8]. The investigation is a wide-ranging experimental study aimed at determining both the details of the flow field and the pressure drop and friction factor characteristics for turbulent flow in eccentric annular ducts. The experiments were performed utilizing three annular ducts of different diameter ratios; in each case the eccentricity was varied from

zero (concentric annulus) to unity (walls in contact). To provide the broadest possible perspective, the measurements of velocity field are presented in three different ways. First, contour maps showing lines of constant velocity are constructed. From these circumferential distributions of the local shear stress on the bounding walls are deduced. Velocity profiles along lines normal to the walls are represented in terms of law-of-the-wall variables and defect-law variables. Neither of these representations affords complete agreement with the universal circular-tube distributions. In general, the defect-law provides a somewhat closer correlation of the results for the eccentric annulus with those for the tube. The experimental findings do not substantiate a prior analytical model, which assumes that the universal law of the wall applies on all lines normal to the bounding walls of the annulus. Friction factors based on the static pressure measurements, are shown to decrease with increasing eccentricity. The measured friction factors are in fair agreement with those of analysis. Hydrodynamic development lengths, deduced from entrance-region pressure data, are found to increase with increasing eccentricity. Circumferential pressure distributions also increase with eccentricity.

Snyder and Goldstein (1965) performed a study on the analysis of fully developed laminar flow in an eccentric annulus [9]. An exact solution of the velocity distribution is presented. From this solution may be obtained expressions for local shear stress on the inner and outer surfaces of the annulus, friction factors based on the inner and outer surfaces, and the overall friction factor. Curves of this data are presented covering a range of eccentricity values and radius ratio values.

Flow of Newtonian and non-Newtonian fluids in concentric and eccentric annuli has been investigated by Nouri, Umur and Whitelaw (1993) [10]. Three components of mean velocity and the corresponding Reynolds shear stresses have been measured in fully developed concentric and eccentric annulus flows of a Newtonian fluid at bulk-flow Reynolds numbers of 8900 and 26600 and a weakly elastic shear-thinning polymer at effective bulk-flow Reynolds numbers of 1150, 6200 and 9600. The diameter ratio was 0.5 with eccentricities of 0, 0.2, 1.0, and the use of a Newtonian fluid of refractive index identical to that of the Perspex working section facilitated the measurements by laser velocimetry.

The problem of the flow across annuli of fine clearance has been investigated both theoretically and experimentally by Tao and Donovan (1954) [11]. The study includes the effects due to the relative motion of the walls and to varying degrees of eccentricity of the bounding surface. The experimental work was carried up to a Reynolds number, based on the diametral clearance, of 30000. The theoretical results are presented both graphically and in the form of equations.

J. Heyda (1959) [12] studied on a Green's function solution for the case of laminar incompressible flow between non-concentric circular cylinders. The main result is the determination of Green's function in bi-polar coordinates for the potential equation for a non-concentric annular region. This is then used to solve

Poisson's equation for the point velocity in laminar incompressible flow between non-concentric circular cylinders.

Axisymmetric flows between counter-rotating cylinders of varying radius ratio are examined by Jones (1982) [13]. The stability of these flows to non-axisymmetric disturbances is considered and the results of these calculations are compared with experiments.

A study on laminar motion of a viscous incompressible fluid between two parallel eccentric cylinders has been investigated by Badr, Farah, Badran (1992) [14]. The flow of incompressible viscous fluid between two eccentric cylinders under the action of a difference between the pressures imposed at the ends of the cylinders is analyzed. Using bipolar coordinates, the resulting boundary value problem is solved analytically, and the average flux velocity is calculated for various values of the geometric parameters of the problem.

A study has been performed by Gravas and Martin (1978) [15] on the instability of viscous axial flow in annuli having a rotating inner cylinder. Hot wire measurements are presented of the onset of instability in developed axial and tangential flow due to inner cylinder rotation in annuli of radius ratios 0.9, 0.81 and 0.58 for axial-flow Reynolds numbers between 86 and 2000.

Stability of axial flow in an annulus with a rotating inner cylinder has been investigated by Lueptow, Docter and Min (1992) [16]. Flow between concentric cylinders with the inner cylinder rotating and an axial pressure gradient imposed in the annulus reveals a rich variety of flow regimes depending on the flow conditions. The occurrence of these flow regimes was studied experimentally by both visually and optically detecting the transition from one regime to another over a wide range of Taylor numbers for moderate axial Reynolds numbers. Seven flow regimes of toroidal vortices were identified including Taylor vortices, wavy vortices, random wavy vortices, modulated wavy vortices, turbulent wavy vortices and turbulent vortices.

Kit and Mazor performed a numerical solution of laminar flow generated in an annulus by rotating screens (1990) [17]. The governing equation and the appropriate boundary condition describing stationary laminar flow in a curved channel and in an annulus with one and two rotating screens, were solved numerically by finite difference method. In the curved channel, multiple solutions were obtained in accordance with the predictions of previous theoretical and experimental investigations. In contrast to that, no multiple solutions were found for the flow in an annulus, neither with two nor with one rotating screen. The numerically computed axial velocity distributions in annulus were compared to the corresponding experimental profiles measured in a turbulent flow of a homogenous fluid created in annulus by one or two rotating screens.

A study on fully developed laminar flow of purely viscous non-Newtonian liquids through annuli, including the effects of eccentricity and inner cylinder rotation has been performed by Escudier, Oliveria and Pinho (2002) [18]. The results are presented of extensive numerical calculations, carried out using a highly accurate finite volume method, for the fully developed laminar flow of an inelastic shear thinning power-law fluid through an eccentric annulus with inner cylinder rotation.

A computational study is performed by Char and Hsu (1998) [19] on two-dimensional mixed convection in an annulus between a horizontal outer cylinder and a heated, rotating, eccentric inner cylinder. The computations have been performed using a non-orthogonal grid and a fully collocated finite volume procedure. The numerical procedure adopted can easily eliminate the numerical leakage phenomenon of the mixed convection problem whereby strong buoyancy and centrifugal effects are encountered in the case of a highly eccentric annulus.

Direct numerical simulation of the turbulent flow in a pipe with annular cross-section is studied for the first time, using the Navier-Stokes equations written in cylindrical coordinates by Quadrio and Luchini (2002) [20]. To this aim a novel numerical method is developed, which extends to the cylindrical coordinate system an existing, efficient method designed for cartesian coordinates, and allows eliminating the pressure and formulating the problem in two scalar unknowns.

T.C. YÜKSEKÖĞRETİM KURULU
DOKÜMANTASYON MERKEZİ

The paper by Raspo, Hugues, Serre, Randriamampiania and Bontoux (2002) [21] presents an efficient projection method to solve the three-dimensional time-dependant incompressible Navier-Stokes equations in primitive variables formulation using spectral approximations. The modified projection method is applied to the simulation of complex three-dimensional flows in rotating cavities, involving either a throughflow or a differential rotation.

Validation of a finite difference method for the simulation of vortex-induced vibrations on a circular cylinder has been done by Wanderley and Levi (2000) [22]. The Karman Vortex Street generated by a circular cylinder is investigated by the numerical solution of the compressible Navier-Stokes equations in the incompressible Mach number range using the Beam and warming implicit scheme. The agreement with the fully incompressible projection method is fairly good while convergence time is very much better. The investigations suggest that the compressible Navier-Stokes equations may be used as an efficient alternative to study incompressible flows as well. Mach numbers just below 0.3 are enough to simulate incompressible flow behavior and at the same time do not cause numerical ill-conditioning in the solution. In addition, some relevant features of the vortices generated and carried by the wake of the cylinder could be fairly well captured.

2.3 Literature related to the numerical method of this study

The paper by Liszka and Orkisz is about the finite difference method at arbitrary irregular grids and its applications in applied mechanics (1980) [23]. Modification of the finite difference method enables local condensation of the mesh and easy discretization of the boundary conditions in the case of an arbitrary shape of the domain. As a result, an essential reduction of the required number of nodal points may usually be achieved. Thus the FDM can be competitive in some fields to the finite element method.

A local interpolation method for an irregular mesh of nodal points is proposed by Liszka (1983) [24]. The method is based on a Taylor expansion of the unknown function combined with the minimization of errors. Some numerical tests as well as a computer program are presented. Applicability and stability of the method are shown in the study. By the appropriate definition of weighting coefficients, this method may be viewed as an interpolation or approximation in the sense of minimum deviation from given values. Applications in finite element and finite difference methods are shown.

Meshless methods are recognized as very efficient methods to solve partial differential equations. In the paper by Gavete and Cuesta (2001) [25], two different meshless methods are considered based on moving least squares method with appropriate weighting functions and areas of influence. The accuracy

obtained using generalized finite difference method (GFD) and element free Galerkin (EFG) method is compared in different domains with irregular and regular clouds of points. Some advantages and main drawbacks of each method are established. GFD method is simpler as compared with EFG method, however solving Laplace equation GFD method is more accurate, particularly in the calculation of the derivatives.

A two dimensional finite difference technique for irregular meshes is formulated for derivatives up to the second order by Perrone and Kaos (1975) [26]. The domain in the vicinity of a given central point is broken into eight 45 degree pie shaped segments and the closest finite difference point in each segment to the center point is noted. By utilizing Taylor series expansions about a central point with a unique averaging process for the points in the four diagonal segments, good approximations to the all derivatives up to the second order and including the mixed derivatives are obtained. For square meshes, the general derivative expressions for arbitrary meshes, which were determined, reduce to the usual finite difference formulae. In one example problem, the Poisson equation is solved for an irregular mesh. In a second example for the first time a problem with a geometric nonlinearity, namely large deflection response of a flat membrane, is solved with an irregular mesh. The solutions compare very favorably with the previously obtained results.

Paper by Benito, Urena and Gavete (2001) [27] is about the influence of several factors in the generalized finite difference method. In the paper it is possible to appreciate the great efficiency of the generalized finite difference method, that is to say with an irregular arrangement of nodes, to solve second order partial differential equations which represent the behavior of many physical processes. The method solves any type of second order differential equation, in any type of domain and boundary condition and immediately obtains the values of derivatives of the nodes through the application of the formulae in differences obtained. This paper analyses the key parameters of the method, such as the number of nodes of the star, the arrangement of the star, the weight function and the stability parameter in time-dependant problems. This analysis includes solutions obtained for different types of problems, represented by different differential equations, including time-dependant equations and under different boundary conditions.

The work by Bonet and Kulasegaram (2002) [28] presents an approach to improve the accuracy and stability of smooth particle hydrodynamics techniques and describes how this correction procedure can be combined with kernel correction to formulate a complete form of the corrected smooth particle hydrodynamics method. The development and theory of this new approach is presented in the context of the solution of Poisson equations. Successful implementation of the theory is verified via various numerical examples.

A numerical method using generalized finite differences and a three dimensional computational model with fluid-wall interactions is introduced to investigate viscous flow in stenotic elastic tubes with large wall deformation and collapse, in the study by Tang, Yang, Kobayashi and Ku (2001) [29]. The Navier-Stokes equations are used as the governing equations for the fluid while a thin-shell theory is used for the wall model. Use of the unstructured GFD method and an incremental boundary iteration technique makes it possible to handle critical flow conditions with large velocity and pressure gradients and fluid-structure interactions with large deformation and wall- collapse.

In the other study by Tang, Yang, Kobayashi and Ku (2001) [30], a numerical method using GFD is introduced to solve nonlinear axisymmetric model with a free moving boundary to study unsteady viscous flow in collapsible stenotic tubes simulating blood flow in stenotic carotid arteries, is investigated. The Navier-Stokes equations are used as the governing equations for the fluid flow.

Boundaries and boundary conditions are an aspect of the numerical solution of partial differential equations where meshless methods have had to surmount many initial difficulties due to the lack of a finite-element-like Kronecker delta condition. Furthermore, it is frequently desirable, especially in fluid mechanics, to impose general, nonlinear boundary and interface constraints.

T.C. YÜKSEKÖĞRETİM KURULU
DOKÜMANTASYON MERKEZİ

The study by Shu and Wee (2002) [31] is the first endeavor whereby the two-dimensional incompressible Navier-Stokes equations in primitive variable form are solved by using the generalized differential quadrature method with SIMPLE strategy. A new approach is proposed to enforce the continuity condition on the boundary and to implement the boundary condition for pressure correction equation. It is demonstrated that accurate numerical results can be obtained by the this method using a few grid points. It is also shown that the multi-stage process can enhance the convergence rate of the numerical simulation.

The stability of a finite difference discretization of the time-dependant incompressible Navier-Stokes equations in Velocity-pressure formulation is studied by Petersson (2001) [32]. In particular, the stability for different pressure boundary conditions in a semi-implicit time integration scheme, where only the viscous term is treated implicitly, is studied.

Amedodji, Bayada and Chambat (2002) have a study on the unsteady Navier-Stokes equations in a time-moving domain with velocity-pressure boundary conditions [33].

A defect-correction method for the incompressible Navier-Stokes equation with a high Reynolds number is considered in the study by Layton, Lee and Peterson (2002) [34]. In the defect step, the artificial viscosity parameter is added to the

Reynolds number as a stability factor, and the residual is taken care of in the correction step.

In the study by Belytschko, Organ and Krongauz (1995) [35], a procedure is developed for coupling meshless methods such as the element-free Galerkin method with finite element methods. The coupling is developed so that continuity and consistency are preserved on the interface elements. Results are presented for both elastostatic and elastodynamic problems, including a crack growth.

A detailed description of the Element Free Galerkin method and its numerical implementation is presented with the goal of familiarizing scientists and engineers with the new computational technique, in the study by Dolbow and Belytschko (1998) [36].

CHAPTER 3

GENERALIZED FINITE DIFFERENCE METHOD

3.1 General

The Navier-Stokes equations, which were described in Chapter 1, are one of the most difficult type of equations to be solved by numerical techniques since they both include convective and diffusive terms for the velocity and a pressure term. The absence of pressure term in the third equation (Equation 1.3), which is continuity, causes the continuity equation to become a constraint for the two components of Navier-Stokes equations (Equations 1.1 and 1.2) given the flow field is 2-D.

The numerical methods applied to the fluid mechanics problems are all well known. The finite difference method has been a powerful tool since the beginning of the era of computational fluid dynamics. But its adaptability to irregular geometries is a rather tough stuff.

Finite volume approach is broadly used in computational fluid mechanics since it is very adaptable to the physical situation. But it also has some shortcomings in

representing derivatives. Another popular method is the finite element method that divides the domain into regular shapes and calculates the properties element wise.

For the last few years a new method is beginning to be used for the solution of partial differential equations. The method is a kind of meshless method, which is known as the generalized finite difference method. The method requires no cells or volumes for the calculation. It is based on a Taylor series expansion of the unknown function combined with the minimization of the errors.

3.2 Numerical Method

The objective of meshless methods is to eliminate at least a part of the structure of elements as in Finite Element Method by constructing the approximation entirely in terms of nodes. Although meshless methods were originated about twenty years ago, the research effort devoted to them until last few years was very small.

One of the starting points is the smooth particle hydrodynamics (SPH) method. Other path in the evolution of meshless methods has been the development of generalized finite difference method (GFD), also called meshless finite difference method. One of the early contributors to the former was Perrone and Kao [26]. The more robust of these methods was developed by Liszka and Orkisz [23],

using a moving least squares approximation. The method proposed by Liszka and Orkisz [23], which will be given in detail in the next section, is used in this study.

3.2.1 Theory

Consider a set of nodes around an arbitrary point P:

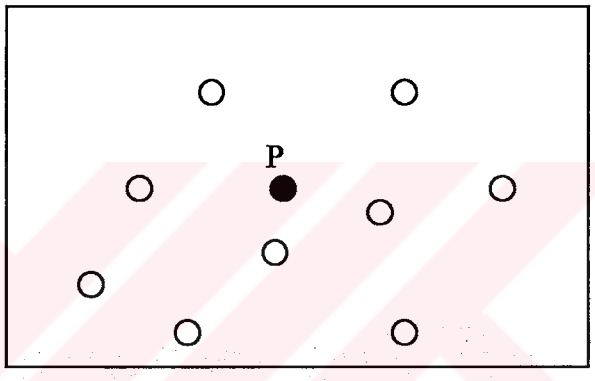

Figure 3.1 A set of points neighboring point P

A Taylor series expansion of any function "f_i" at the rest of the nodes around point $P(x_0,y_0)$ can be expressed in the form given in Equation 3.1.

$$f_i(x+h_i,y+k_i)=f_0+h_i\frac{\partial f_0}{\partial x}+k_i\frac{\partial f_0}{\partial y}+\frac{h_i^2}{2}\frac{\partial^2 f_0}{\partial x^2}+\frac{k_i^2}{2}\frac{\partial^2 f_0}{\partial y^2}+h_ik_i\frac{\partial^2 f_0}{\partial x\partial y}+o(\rho^3) \quad (3.1)$$

where:

$i=1..n$; and n is the number of nodes and

$h_i = x_i - x_0$ $k_i = y_i - y_0$

(x_0 , y_0) are the coordinates of point P, (x_i , y_i) are the coordinates of the i^{th} node.

If we ignore the high order terms in Equation 3.1, an approximation of the f_i function is obtained. This expression is valid for i = 1 to n and subsequently, all these expressions may be added in order to obtain Equation 3.2.

$$\sum_{i=1}^{n}(f_i - f_0)=\sum_{i=1}^{n}h_i\frac{\partial f_0}{\partial x}+\sum_{i=1}^{n}k_i\frac{\partial f_0}{\partial y}+\frac{1}{2}(\sum_{i=1}^{n}h_i^2\frac{\partial^2 f_0}{\partial x^2}+\sum_{i=1}^{n}k_i^2\frac{\partial^2 f_0}{\partial y^2}+\sum_{i=1}^{n}2h_ik_i\frac{\partial^2 f_0}{\partial x\partial y}) \quad (3.2)$$

It is then possible to define norm B in the following manner:

$$B=\sum_{i=1}^{n}\left[\left[f_0 - f_i + h_i\frac{\partial f_0}{\partial x}+k_i\frac{\partial f_0}{\partial y}+\frac{h_i^2}{2}\frac{\partial^2 f_0}{\partial x^2}+\frac{k_i^2}{2}\frac{\partial^2 f_0}{\partial y^2}+h_ik_i\frac{\partial^2 f_0}{\partial x\partial y}\right]w_i\right]^2 \quad (3.3)$$

where w_i is the weight function and f (x , y) is a function at least two times differentiable.

As in the classic finite difference case, the idea is to transform the equations of the problem into a series of linear equations where the unknowns f (x_i , y_i) are the values of the function f (x ,y) within a set of n points of the domain, referred to as nodes. As in the classic method, a linear equation is obtained for each node and, subsequently, for each associated group of nodes. As such it is necessary to find

expressions, which transform the partial derivatives into linear expressions of the values of function in the group of nodes.

If the norm B is minimized with respect to $\partial f_0/\partial x, \partial f_0/\partial y, \partial^2 f_0/\partial x^2$, $\partial^2 f_0/\partial y^2, \partial^2 f_0/\partial x\partial y$ and if these derivatives are indicated as α, β, γ, δ, ε, respectively, the following equations are obtained:

$$\frac{\partial B}{\partial \alpha} = 2\sum_{i=1}^{n} \Phi w_i h_i w_i = 0 \tag{3.4}$$

$$\frac{\partial B}{\partial \beta} = 2\sum_{i=1}^{n} \Phi w_i k_i w_i = 0 \tag{3.5}$$

$$\frac{\partial B}{\partial \gamma} = 2\sum_{i=1}^{n} \Phi w_i \frac{h_i^{\,2} w_i}{2} = 0 \tag{3.6}$$

$$\frac{\partial B}{\partial \delta} = 2\sum_{i=1}^{n} \Phi w_i \frac{k_i^{\,2} w_i}{2} = 0 \tag{3.7}$$

$$\frac{\partial B}{\partial \varepsilon} = 2\sum_{i=1}^{n} \Phi w_i h_i k_i w_i = 0 \tag{3.8}$$

where:

$$\Phi = \left[f_0 - f_i + h_i \frac{\partial f_0}{\partial x} + k_i \frac{\partial f_0}{\partial y} + \frac{h_i^2}{2} \frac{\partial^2 f_0}{\partial x^2} + \frac{k_i^2}{2} \frac{\partial^2 f_0}{\partial y^2} + h_i k_i \frac{\partial^2 f_0}{\partial x \partial y} \right] \qquad (3.9)$$

This then gives a set of five linear equations with five unknowns (α, β, γ, δ, ε) which when solved provide the explicit equations of the unknowns in terms of the value of function f of all the nodes in the group of nodes, the values of h_i, k_i, and the weight function w_i.

Although there are several alternatives like exponential or cubic spline weight functions, The recommended and most widely used weight function is used which is $1/d_i^3$ for each node, where d_i is the distance between point P and i^{th} node.

The system may be expressed in matrix form as in Equation 3.10:

$$\begin{bmatrix} \sum w_i^2 h_i^2 & \sum w_i^2 h_i k_i & \sum w_i^2 \frac{h_i^3}{2} & \sum w_i^2 \frac{k_i^2 h_i}{2} & \sum w_i^2 h_i^2 k_i \\ \sum w_i^2 h_i k_i & \sum w_i^2 k_i^2 & \sum w_i^2 \frac{h_i^2 k_i}{2} & \sum w_i^2 \frac{k_i^3}{2} & \sum w_i^2 h_i k_i^2 \\ \sum w_i^2 \frac{h_i^3}{2} & \sum w_i^2 \frac{h_i^2 k_i}{2} & \sum w_i^2 \frac{h_i^4}{4} & \sum w_i^2 \frac{h_i^2 k_i^2}{4} & \sum w_i^2 \frac{h_i^3 k_i}{2} \\ \sum w_i^2 \frac{k_i^2 h_i}{2} & \sum w_i^2 \frac{k_i^3}{2} & \sum w_i^2 \frac{h_i^2 k_i^2}{4} & \sum w_i^2 \frac{k_i^4}{4} & \sum w_i^2 \frac{k_i^3 h_i}{2} \\ \sum w_i^2 h_i^2 k_i & \sum w_i^2 h_i k_i^2 & \sum w_i^2 \frac{h_i^3 k_i}{2} & \sum w_i^2 \frac{k_i^3 h_i}{2} & \sum w_i^2 h_i^2 k_i^2 \end{bmatrix} \begin{Bmatrix} \frac{\partial f_0}{\partial x} \\ \frac{\partial f_0}{\partial y} \\ \frac{\partial^2 f_0}{\partial x^2} \\ \frac{\partial^2 f_0}{\partial y^2} \\ \frac{\partial^2 f_0}{\partial x \partial y} \end{Bmatrix} = \begin{pmatrix} -f_0 \sum w_i^2 h_i + \sum f_i w_i^2 h_i \\ -f_0 \sum w_i^2 k_i + \sum f_i w_i^2 k_i \\ -f_0 \sum w_i^2 \frac{h_i^2}{2} + \sum f_i w_i^2 \frac{h_i^2}{2} \\ -f_0 \sum w_i^2 \frac{k_i^2}{2} + \sum f_i w_i^2 \frac{k_i^2}{2} \\ -f_0 \sum w_i^2 h_i k_i + \sum f_i w_i^2 h_i k_i \end{pmatrix} \qquad (3.10)$$

The above system can be written as:

$$A \times Df = F \tag{3.11}$$

where:

$$A = \begin{bmatrix} \sum w_i^2 h_i^2 & \sum w_i^2 h_i k_i & \sum w_i^2 \frac{h_i^3}{2} & \sum w_i^2 \frac{k_i^2 h_i}{2} & \sum w_i^2 h_i^2 k_i \\ \sum w_i^2 h_i k_i & \sum w_i^2 k_i^2 & \sum w_i^2 \frac{h_i^2 k_i}{2} & \sum w_i^2 \frac{k_i^3}{2} & \sum w_i^2 h_i k_i^2 \\ \sum w_i^2 \frac{h_i^3}{2} & \sum w_i^2 \frac{h_i^2 k_i}{2} & \sum w_i^2 \frac{h_i^4}{4} & \sum w_i^2 \frac{h_i^2 k_i^2}{4} & \sum w_i^2 \frac{h_i^3 k_i}{2} \\ \sum w_i^2 \frac{k_i^2 h_i}{2} & \sum w_i^2 \frac{k_i^3}{2} & \sum w_i^2 \frac{h_i^2 k_i^2}{4} & \sum w_i^2 \frac{k_i^4}{4} & \sum w_i^2 \frac{k_i^3 h_i}{2} \\ \sum w_i^2 h_i^2 k_i & \sum w_i^2 h_i k_i^2 & \sum w_i^2 \frac{h_i^3 k_i}{2} & \sum w_i^2 \frac{k_i^3 h_i}{2} & \sum w_i^2 h_i^2 k_i^2 \end{bmatrix}$$

$$Df = \begin{Bmatrix} \frac{\partial f_0}{\partial x} \\ \frac{\partial f_0}{\partial y} \\ \frac{\partial^2 f_0}{\partial x^2} \\ \frac{\partial^2 f_0}{\partial y^2} \\ \frac{\partial^2 f_0}{\partial x \partial y} \end{Bmatrix} \quad \text{and} \quad F = \begin{bmatrix} -f_0 \sum w_i^2 h_i + \sum f_i w_i^2 h_i \\ -f_0 \sum w_i^2 k_i + \sum f_i w_i^2 k_i \\ -f_0 \sum w_i^2 \frac{h_i^2}{2} + \sum f_i w_i^2 \frac{h_i^2}{2} \\ -f_0 \sum w_i^2 \frac{k_i^2}{2} + \sum f_i w_i^2 \frac{k_i^2}{2} \\ -f_0 \sum w_i^2 h_i k_i + \sum f_i w_i^2 h_i k_i \end{bmatrix}$$

Then the system can be rearranged and simplified as shown in Equation 3.12.

$$A_{5\times5} \times Df_{5\times1} = G_{5\times n} \times f_{n\times1} \tag{3.12-a}$$

$$Df_{5\times1} = A^{-1}_{5\times5} \times G_{5\times n} \times f_{n\times1} \qquad (3.12\text{-b})$$

where:

$$G = \begin{bmatrix} w_1h_1 & w_2h_2 & ..... & \sum w_ih_i & ..... & w_nh_n \\ w_1k_1 & w_2k_2 & ..... & \sum w_ik_i & ..... & w_nk_n \\ \frac{w_1h_1^{\,2}}{2} & \frac{w_2h_2^{\,2}}{2} & ..... & \sum w_i\frac{h_i^{\,2}}{2} & ..... & w_n\frac{h_n^{\,2}}{2} \\ \frac{w_1k_1^{\,2}}{2} & \frac{w_2k_2^{\,2}}{2} & ..... & \sum w_i\frac{k_i^{\,2}}{2} & ..... & w_n\frac{k_n^{\,2}}{2} \\ w_1h_1k_1 & w_2h_2k_2 & ..... & \sum w_ih_ik_i & ..... & w_nh_nk_n \end{bmatrix}$$

Column for node at point P

and $f^T = [f_1 \quad f_2 \quad ..... \quad f_n]$

Equation 3.12 can be rewritten as:

$$Df_{5\times1} = C_{5\times n} \times f_{n\times1} \qquad (3.13)$$

where $C_{5\times n} = A^{-1}_{5\times5} \times G_{5\times n}$

So all the derivatives are expressed in terms of unknown function values at nodal points. Writing the equation above for all nodes yields n equations for n unknown

function values. Knowing the five derivatives in terms of function values we are able to find a solution for a differential equation.

3.2.2 Advantages of the Method

Some of the advantages of the method can be outlined as:

- It is a one stage, local procedure method.
- Easy calculation for an arbitrarily irregular group of nodes is possible.
- Stable results are obtained.
- The method is also suitable for extrapolation outside the domain.
- Inserting extra nodes at any step of the calculation does not cause any problem.
- Boundary conditions are successfully represented.
- More accurate results can be obtained.

CHAPTER 4

COMPUTER PROGRAM

4.1 Structure of the Program

The computer program is composed of a main program that solves the vorticity transport equation in an iterative manner by lagging the velocity components in the convective terms- so that a linear equation for vorticity transport equation is obtained- a subprogram that builds expressions for derivative components and a solver that solves the system of equations. The code is given in Appendix A.

The main program firstly builds the coordinates of each node in the domain for a given geometry. i.e. the inner and outer radius of circles, the eccentricity and the number of nodes to be generated.

The node structure is built by putting circles with varying radius and eccentricities and putting nodes on these circles at certain angles. As an example of is given on Figure 4.1 for 60% eccentricity.

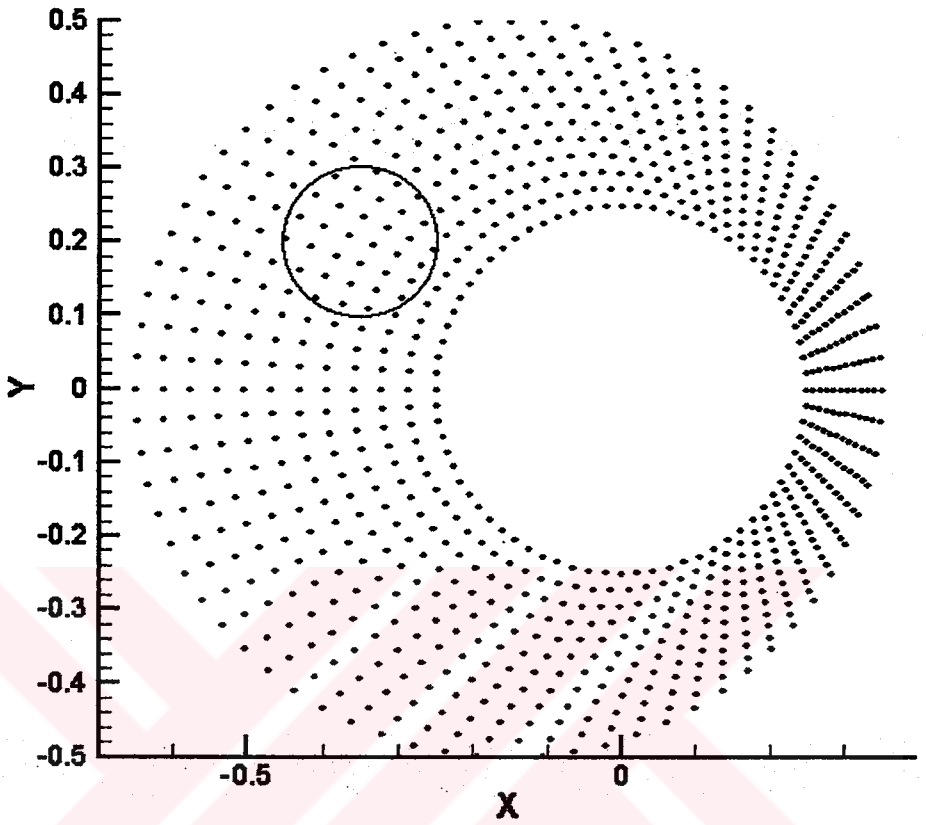

Figure 4.1 The node structure built for 60% eccentricity

The set of nodes shown in Figure 4.1 is composed of 864 nodes for which 12 nodes are aligned in radial direction and vary with 5 degrees with respect to the center of the circles with varying eccentricities from 0 (i.e. the inner circle) to 60% (i.e. the outer circle).

Secondly, for the known coordinates of nodes, the main program calls the subroutine for a node, builds the derivative expressions by meshless algorithm and

stores the right hand side (matrix A_{5x5} in equation 3.12a) and left hand side (matrix B_{5xn} in equation 3.12a) matrices for that node. Then the output matrix A_{5x5} of the meshless subroutine is inversed by a second subroutine that performs the inversing operation of a square matrix. The obtained A^{-1}_{5x5} matrix is multiplied with B_{5xn} matrix to obtain the five derivative expressions of that node in a C_{5xn} matrix given in equation 3.13. The C_{5xn} matrix for the given node, say node number P, is stored in a global matrix of dimension nx5xn at the P^{th} location of the first dimension of the global matrix. Then the procedure is repeated for each node in the domain and the C_{5xn} matrices are stored in the global matrix for each node.

4.2 Subroutines of the Program

The subroutine of meshless method calculates derivatives by Taylor series expansions, weights the residuals and minimizes the expression by taking derivatives with respect to each derivative components $\alpha, \beta, \gamma, \delta, \varepsilon$, given in equations 3.4 through 3.8. The important point is to choose the points, which will effect the derivative at a given point P.

Since the weight function w_i will diminish with increasing distance, the effect of the points far from the point P will also diminish. In order to reduce the number of calculations and not to introduce errors caused by very small numbers (i.e. $1x10^{-9}$)

T.C. YÜKSEKÖĞRETİM KURULU
DOKÜMANTASYON MERKEZİ

in inversing operations, such points are not included in the calculation of derivatives for that node.

Several methods were proposed in the literature including the distance criterion, four segment criterion, eight segment criterion etc. The evaluation of each criterion can be found in Benito, et.al., [27].

In this thesis a structured configuration of nodes is selected. The selection of nodes from the circled area in Figure 4.1 is given in Figure 4.2.

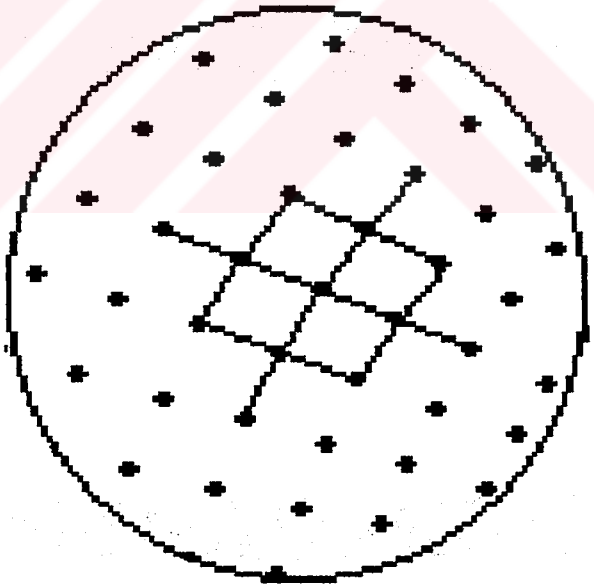

Figure 4.2 The selection of nodes

The nodes affecting the central node are shown on Figure 4.2. Since there are 5 unknown derivative expressions 5 node is needed for minimization. There are 12 nodes affecting the central node P such that the weights of the other nodes were taken as zero.

4.3 Formulation of the Problem

The program builds all the derivative expressions up to now for the given geometric properties. The two dimensional incompressible Navier-Stokes equations are represented by two alternative formulations.

The first one is the primitive variables (u-v-p) formulation as given in equations 1.1 through 1.3. The second formulation is the vorticity stream function formulation. In this thesis, the system of equations is built for the vorticity stream function formulation.

4.3.1 Primitive Variables (u-v-p) Formulation

There are several difficulties when the problem is handled by primitive variables formulation. The main problem is that there is no explicit transport equation for pressure. Although the pressure gradient term appears in the momentum equations, there is no apparent equation to solve for pressure. Therefore special

techniques are required to solve the primitive variable form of the incompressible Navier-Stokes equations.

The SIMPLE algorithm and its various versions are such techniques. These methods are essentially iterative guess and correct procedures. Generally, they consist of solving the momentum equations by using a guessed pressure field to obtain an intermediate velocity field. Then the pressure-correction equation, which is obtained using the continuity equation, is solved using the intermediate velocities. Then the velocities and the pressures are corrected using the pressure-correction. The process is repeated until the continuity is satisfied.

The second limitation is that, there is no specific boundary condition for pressure and pressure correction. Another technique is to solve the three equations simultaneously. But this results in a huge system of equations that is very uneconomic to solve.

4.3.2 Vorticity-Stream Function (ζ-ψ) Formulation

The second formulation is the vorticity stream function formulation. In this thesis, the system of equations is built for the vorticity stream function formulation. This method solves one parabolic (vorticity transport equation) and one elliptic (Poisson equation for stream function) equation. The formulation is advantageous because no pressure term appears in the formulation and solving the equation for

stream function with proper boundary conditions automatically satisfies continuity.

For a 2-D incompressible, viscous flow in x-y plane the flow characteristics can be represented by vorticity transport equation.

$$\frac{\partial \zeta}{\partial t} + u\frac{\partial \zeta}{\partial x} + v\frac{\partial \zeta}{\partial y} = \upsilon\left(\frac{\partial^2 \zeta}{\partial x^2} + \frac{\partial^2 \zeta}{\partial y^2}\right) \tag{4.1}$$

Where ζ is the vorticity, υ is the viscosity of the fluid, u and v are the velocity vectors in x and y directions respectively. And the vorticity is defined as:

$$\zeta = \frac{\partial v}{\partial x} - \frac{\partial u}{\partial y} \tag{4.2}$$

Then the velocity components can be written in terms of stream function:

$$u = \frac{\partial \psi}{\partial y} \tag{4.3}$$

$$v = -\frac{\partial \psi}{\partial x} \tag{4.4}$$

A poisson equation for stream function can be obtained from the definition of vorticity by inserting equation 4.3 and 4.4 into equation 4.2.

$$\frac{\partial^2 \psi}{\partial x^2} + \frac{\partial^2 \psi}{\partial y^2} = -\zeta \tag{4.5}$$

The equations 4.1 and 4.5 are solved in an iterative manner. The velocities in the nonlinear convective terms in vorticity transport equation are lagged in the formulation. A first order forward finite difference is applied to the time derivative for vorticity as shown in equation 4.6.

$$\frac{\partial \zeta}{\partial t} = \frac{\zeta^{k+1} - \zeta^{k}}{\Delta t} \tag{4.6}$$

A fully implicit scheme is applied and all the space derivatives are calculated at k+1 time level. The Space derivatives are calculated by generalized finite difference method as explained in Chapter 3.

Consider the vorticity transport equation, written at node P. The time derivative is calculated using equation 4.6. The C_{5xn} matrix for node P represents all the derivatives and each derivate (i.e. x, y, x^2, y^2, xy) is stored on the rows of the C_{5xn} matrix.

If $\underline{\zeta}$ is the vector ζ containing all the nodal ζ_i values the x derivative is represented as the multiplication of the first row of C_{5xn} matrix with vorticity vector ($\underline{\zeta}$).

$$\frac{\partial \zeta}{\partial x} = C^{1^{st}\,row} \cdot \underline{\zeta} \tag{4.7-a}$$

or

$$\frac{\partial \zeta}{\partial x} = \sum_{i=1}^{n} C_{1,i} \cdot \zeta_i \tag{4.7-b}$$

or in vector form:

$$\frac{\partial \zeta}{\partial x} = \begin{bmatrix} c_{1,1} & c_{1,2} & \cdots\cdots\cdots & c_{1,n} \end{bmatrix} \cdot \begin{bmatrix} \zeta_1 \\ \zeta_2 \\ \vdots \\ \zeta_n \end{bmatrix} \tag{4.7-c}$$

Where n is the total number of nodes in the system. Similarly, the other derivatives can be shown as follows:

$$\frac{\partial \zeta}{\partial y} = \sum_{i=1}^{n} C_{2,i} \cdot \zeta_i \tag{4.8}$$

$$\frac{\partial^2 \zeta}{\partial x^2} = \sum_{i=1}^{n} C_{3,i} \cdot \zeta_i \tag{4.9}$$

$$\frac{\partial^2 \zeta}{\partial y^2} = \sum_{i=1}^{n} C_{4,i} \cdot \zeta_i \tag{4.10}$$

The transport equation at point P is calculated as:

$$\frac{\zeta_p^{k+1} - \zeta_p^{k}}{\Delta t} + u^n \cdot \sum_{i=1}^{n} C_{1,i} \cdot \zeta_i + v^n \cdot \sum_{i=1}^{n} C_{2,i} \cdot \zeta_i = \upsilon \cdot \left(\sum_{i=1}^{n} C_{3,i} \cdot \zeta_i + \sum_{i=1}^{n} C_{4,i} \cdot \zeta_i \right) \tag{4.11}$$

Since all the space derivatives are calculated at time level k+1, the equation is fully implicit. The only term at time level t is the vorticity value at point P. Multiplying the summations with velocity and viscosity values then multiplying all the terms with Δt, the vorticity transport equation is obtained.

The coefficients of each vorticity (ζ_i) value can be written in vector form as follows:

$$\begin{bmatrix} a_1^{\,p} & a_2^{\,p} & \cdots\cdots & a_n^{\,p} \end{bmatrix} \cdot \begin{bmatrix} \zeta_1 \\ \zeta_2 \\ \vdots \\ \zeta_n \end{bmatrix}^{k+1} = \zeta_p^{\,k} \tag{4.12}$$

T.C. YÜKSEKÖĞRETİM KURULU
DOKÜMANTASYON MERKEZİ

where a_i^P represent the effect of i^{th} vorticity value for point P.

Equation 4.12 represents the vorticity transport equation written at point P in vector form. For each of the nodes in the domain (except boundary nodes), a vector equation similar to equation 4.12 for that node can be written. This results in a system of m equations with n unknowns.

If the number of boundary nodes in the system is l,

then m = n-l.

$$\begin{bmatrix} a_1^1 & a_2^1 & \dots & a_n^1 \\ a_1^2 & a_2^2 & \dots & a_n^2 \\ \vdots & \vdots & \vdots & \vdots \\ a_1^m & a_2^m & \dots & a_n^m \end{bmatrix} \cdot \begin{bmatrix} \zeta_1 \\ \zeta_2 \\ \vdots \\ \zeta_n \end{bmatrix}^{k+1} = \begin{bmatrix} \zeta_1 \\ \zeta_2 \\ \vdots \\ \zeta_m \end{bmatrix}^{k} \qquad (4.13)$$

k equation is needed to solve the system. These equations come from the boundary conditions.

The boundary conditions for vorticity can be evaluated from the definition of vorticity. Since the wall is curved no term drops out from the system and rewriting equation 4.2 in terms of summations yields:

$$\zeta = \frac{\partial v}{\partial x} - \frac{\partial u}{\partial y} = \sum_{i=1}^{n} C_{1,i} \cdot v_i - \sum_{i=1}^{n} C_{2,i} \cdot u_i \qquad (4.14)$$

The velocities in equation 4.14 are known for time level t, so the equation 4.14 yields the boundary (wall) value for the vorticity. The equation 4.14 can also be written in vector form. This can be achieved by inserting the value 1 in the diagonal of the square matrix and zero values for other elements. The right hand side of the corresponding equation for boundary is the value calculated from equation 4.14. Then the system is n equations with n unknowns and is ready to be solved.

$$\overline{A} \cdot \tilde{\zeta} = \tilde{L} \qquad (4.15)$$

where $\overline{A}$ is an n by n matrix $\tilde{\zeta}$ a vector containing the unknown values for vorticity and $\tilde{L}$ is the load vector of the system obtained from equation 4.12 and 4.14.

The system is solved by a subroutine called DLSARG. The routine solves a real general system of linear equations with iterative refinement. It first computes the LU factorization of the coefficient matrix and estimate the condition number of the matrix then the solution of the linear system is found using an iterative refinement routine.

In order to solve the system of equations given in equation 4.14, the stream function values can be calculated by solving a Poisson type of equation given in equation 4.5 with the vorticity values calculated.

A similar system to equation 4.15 can be calculated. The second derivatives for stream function (ψ) for node P can be given as:

$$\frac{\partial^2 \psi}{\partial x^2} = \sum_{i=1}^{n} C_{3,i} \cdot \psi_i \tag{4.16}$$

where C is the coefficient matrix of node P same as equation 4.9. Similarly the second derivative with respect to y can be written as:

$$\frac{\partial^2 \psi}{\partial y^2} = \sum_{i=1}^{n} C_{4,i} \cdot \psi_i \tag{4.17}$$

Inserting equation 4.16 and 4.17 into equation 4.5 gives equations for internal nodes.

The boundary conditions must be specified in order to complete the system of equations. The outer boundary is a wall; so a constant value can be given since a solid boundary itself is a streamline.

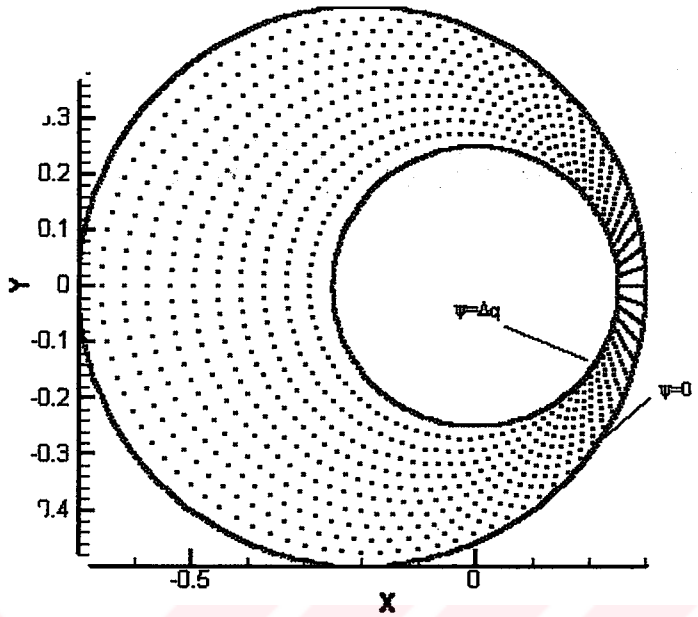

Figure 4.3 Boundary conditions for streamlines

As shown in Figure 4.3, $\psi = 0$ boundary condition is used. The inner boundary itself is also a solid boundary and $\psi =$ constant boundary condition should be implied. But the value of this constant is not known since its value is related to the discharge passing between these two streamlines. From the definition of the streamlines a relation can be written.

$$\psi_{inner} - \psi_{outer} = \Delta q \tag{4.18}$$

ψ_{outer} is taken as zero in the thesis, as explained above. Therefore, $\psi_{inner} = \Delta q$ boundary condition must be employed at the inner boundary. The discharge value can be estimated from velocities found at the previous time level. If the system

converges to a solution, the discharge must also converge to a constant value (i.e. the real value for the inner wall).

With the boundary values calculated again, a system of equations is going to be solved by the routine DLSARG. Now that we have the stream function values for all nodes. We can easily calculate the velocity field by:

$$u = \frac{\partial \psi}{\partial y} \tag{4.19}$$

$$v = -\frac{\partial \psi}{\partial x} \tag{4.20}$$

The velocities at each node are calculated from equations 4.19 and 4.20. Using the known velocities, the wall vorticity values can be calculated so that the iterative procedure starts.

The program is iterated in time until the steady state solution is reached. As the scheme is fully implicit in time, it must be stable for all Δt values. But this is not the case. The boundary conditions are dependent on the calculated velocity fields at each time step. So using large Δt values may overshoot the solution and even no solution may be obtained.

In the case studies several different Δt values are tried. It is seen that for different eccentricities and node numbers, the system fails at different Δt levels. It is also seen that Courant stability condition is safe enough to have a stable condition.

Actually, for low eccentricity values, the system is stable even for 10 times the value found from the Courant stability condition but not for high eccentricity values. So through out the thesis the Courant stability condition is used. The Courant number can be given as:

$$c_r = \frac{u \cdot \Delta t}{\Delta x} \tag{4.21}$$

and to have a stable solution:

$c_r \leq 1$

CHAPTER 5

CASE STUDIES

5.1 Input parameters

The program is executed for several different data sets. The main input parameters to the program can be given as follows:

5.1.1 Geometric parameters:

The geometric parameters are the parameters defining the physical limitations or constraints of the system. These are:

R_{outer}: is the radius of the outer cylinder. The outer radius is taken as 0.5 meters in all case studies.

R_{inner}: is the radius of the inner cylinder. The inner radius is taken as 0.25 meters in all case studies.

Ecc: is the eccentricity between the centers of the cylinder. The minimum value is zero, which corresponds to the concentric case. The value of eccentricity can range between the 0 and 0.25 meters. The fully (100%) eccentric case correspond to the value 'Router-Rinner', which is 0.25 meters. In the case studies 0%, 20%, 40%, 60%, 80% of eccentricities are given as input values. These values correspond to the 0, 0.05, 0.10, 0.15, 0.20 meters of eccentricity.

Omega1 (ω_1): is the angular velocity of the inner cylinder. A range of values from 0.004 to 0.016 is studied in case studies in order to have a range of Reynolds number from 250 to 1000.

Omega2 (ω_2): is the angular velocity of the outer cylinder. It is taken as zero since the outer cylinder corresponds to the casing in drilling machines that is stationary.

5.1.2 Flow parameters:

The flow parameters are the basic characteristics of the flow and the fluid.

Dynamic Viscosity (μ): is taken as an approximate value of 1.0 E-3 in the case studies. It is 1.12 E-3 N.s/m^2 for water but the approximate value is taken in order to have a Reynolds number without decimal places.

T.C. YÜKSEKÖĞRETİM KURULU
DOKÜMANTASYON MERKEZİ

Kinematic Viscosity (υ): is taken as 1.0 E-6 in case studies. It is 1.12 E-6 m^2/s for water.

Density (ρ): is the density of the fluid in kg/m^3. It is taken as 999, the actual value for water.

The Reynolds number is defined as:

$$\mathrm{Re} = \frac{V \cdot D}{\upsilon} \tag{5.1}$$

Where V is the velocity, D is the hydraulic radius and υ is the kinematic viscosity. For the 2-D rotational flow with inner cylinder rotation the representative Reynolds number of the system can be given as:

$$\mathrm{Re} = \frac{\omega_1 \cdot R_{inner} \cdot R_{inner}}{\upsilon} = \frac{\omega_1 \cdot R_{inner}^{\,2}}{\upsilon} \tag{5.2}$$

Where the parameters involved is defined above.

20 Cases for the afore mentioned values of eccentricity and four different values of Reynolds number (250, 500, 750, 1000) are carried out. Characteristics of these

cases are listed in table 5.1. The outputs are the streamline plots and the velocity fields. Graphs for streamlines and vector fields are given for each case.

Table 5.1 Case studies

Ecc / Re	0	20%	40%	60%	80%
250	Case 1	Case 2	Case 3	Case 4	Case 5
500	Case 6	Case 7	Case 8	Case 9	Case 10
750	Case 11	Case 12	Case 13	Case 14	Case 15
1000	Case 16	Case 17	Case 18	Case 19	Case 20

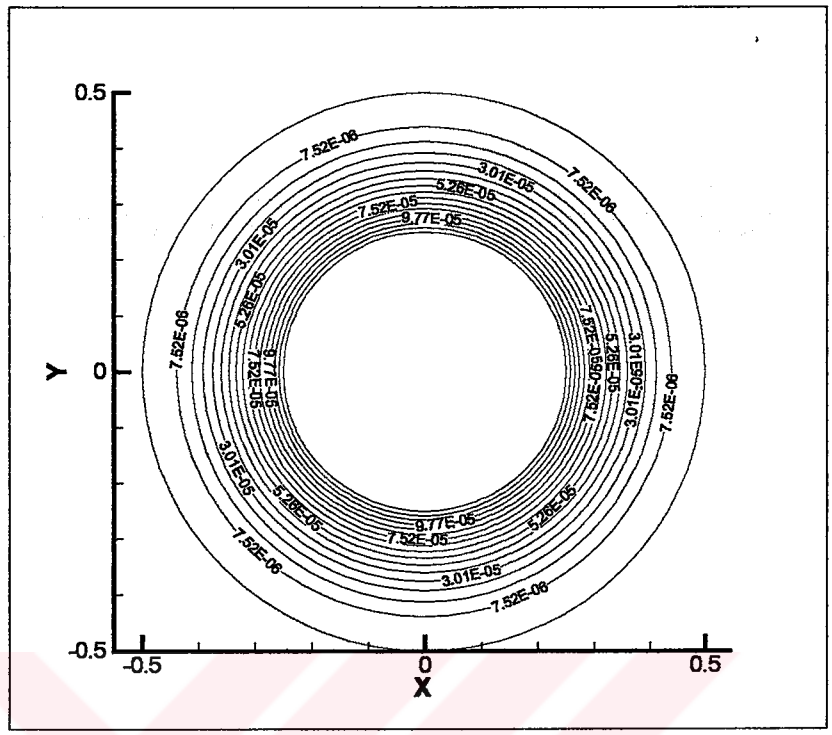

Figure 5.1 Streamline plot for case 1

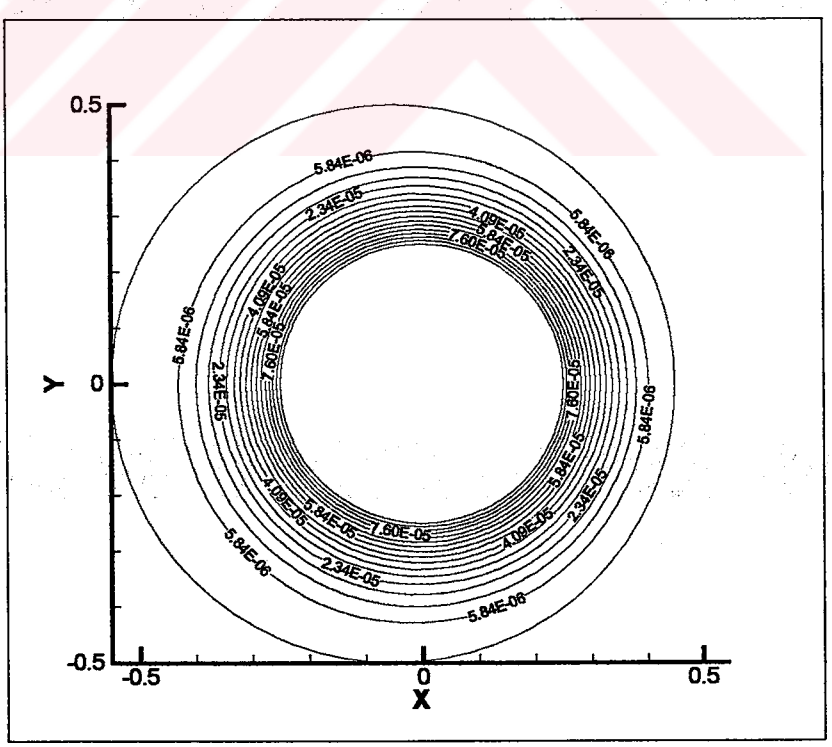

Figure 5.2 Streamline plot for case 2

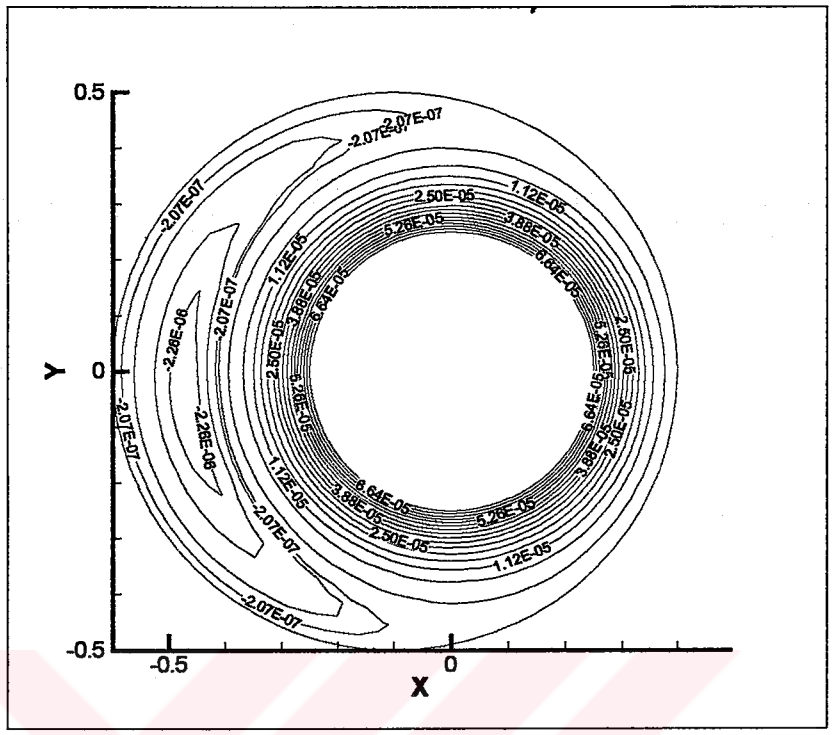

Figure 5.3 Streamline plot for case 3

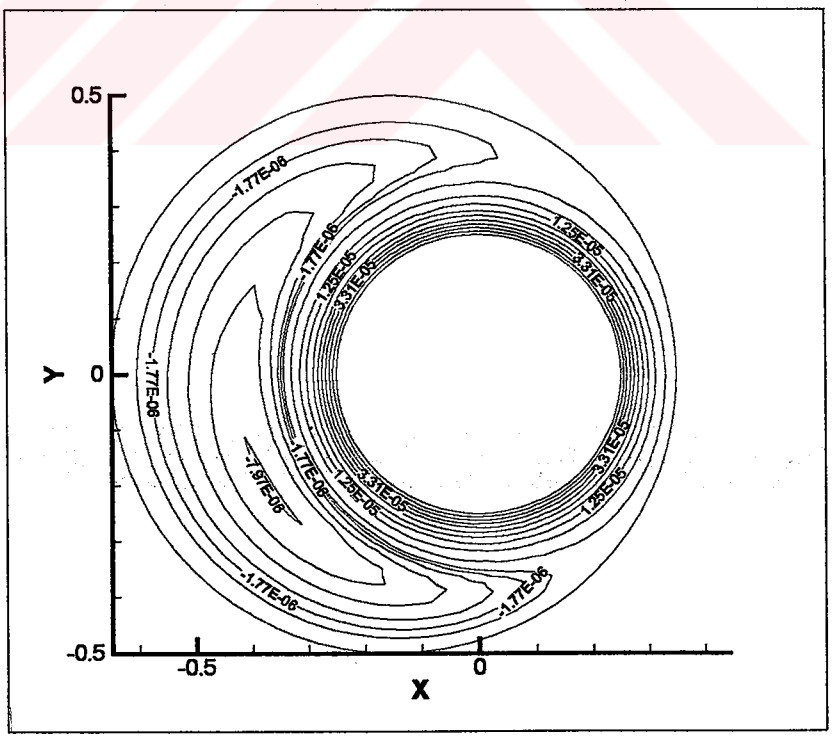

Figure 5.4 Streamline plot for case 4

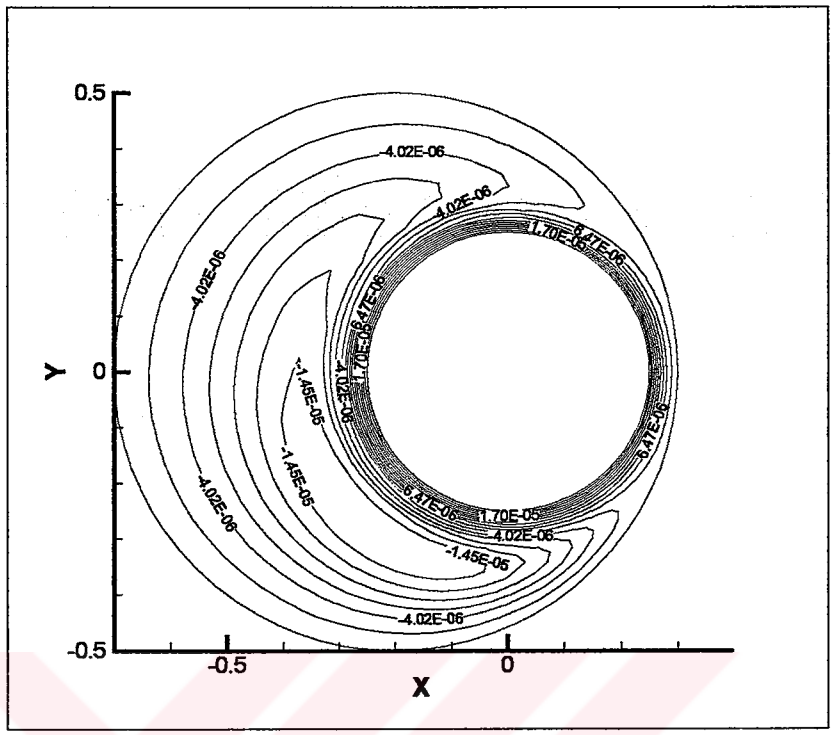

Figure 5.5 Streamline plot for case 5

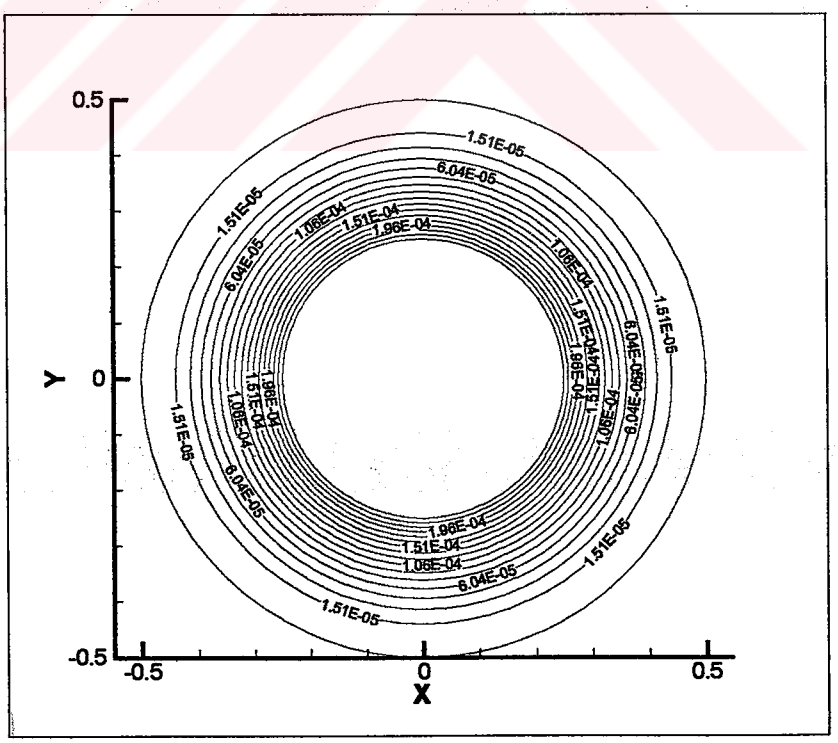

Figure 5.6 Streamline plot for case 6

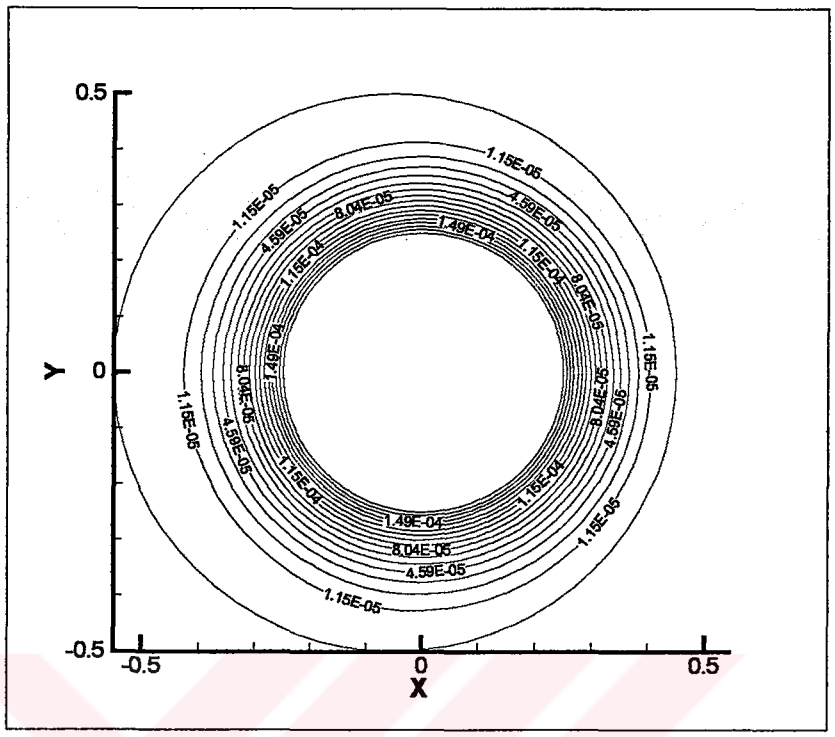

Figure 5.7 Streamline plot for case 7

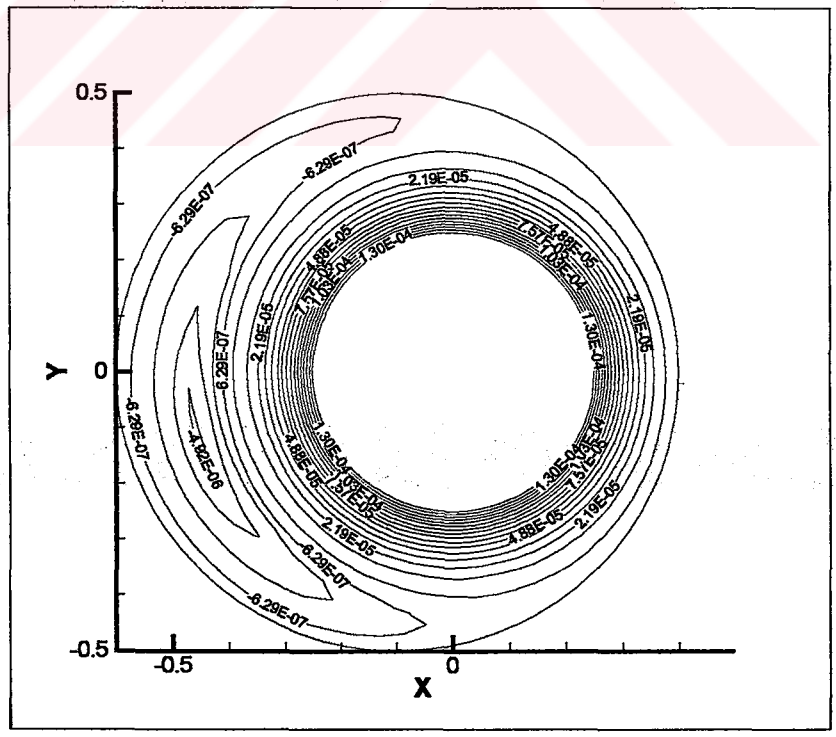

Figure 5.8 Streamline plot for case 8

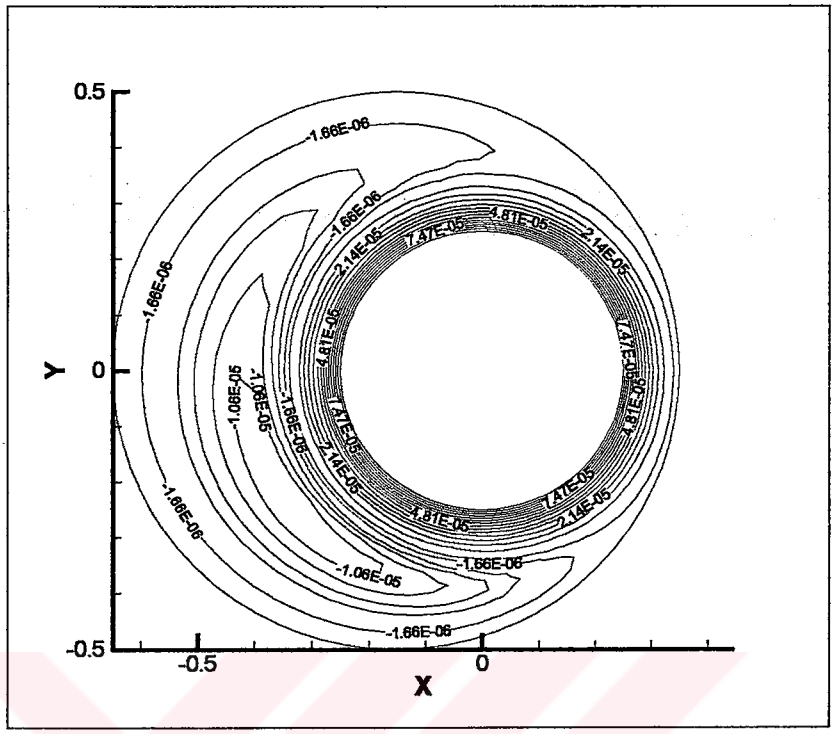

Figure 5.9 Streamline plot for case 9

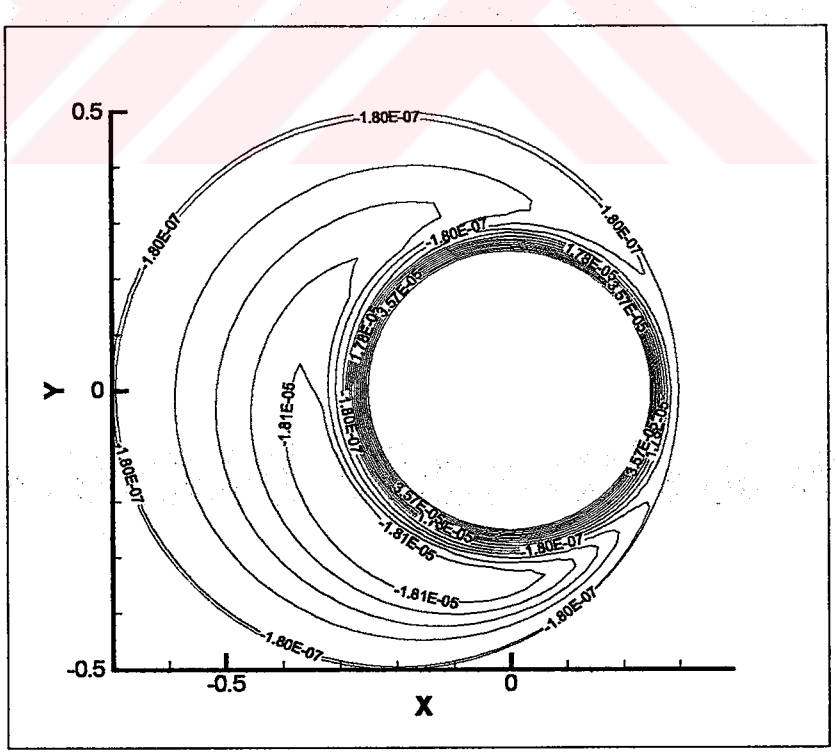

Figure 5.10 Streamline plot for case 10

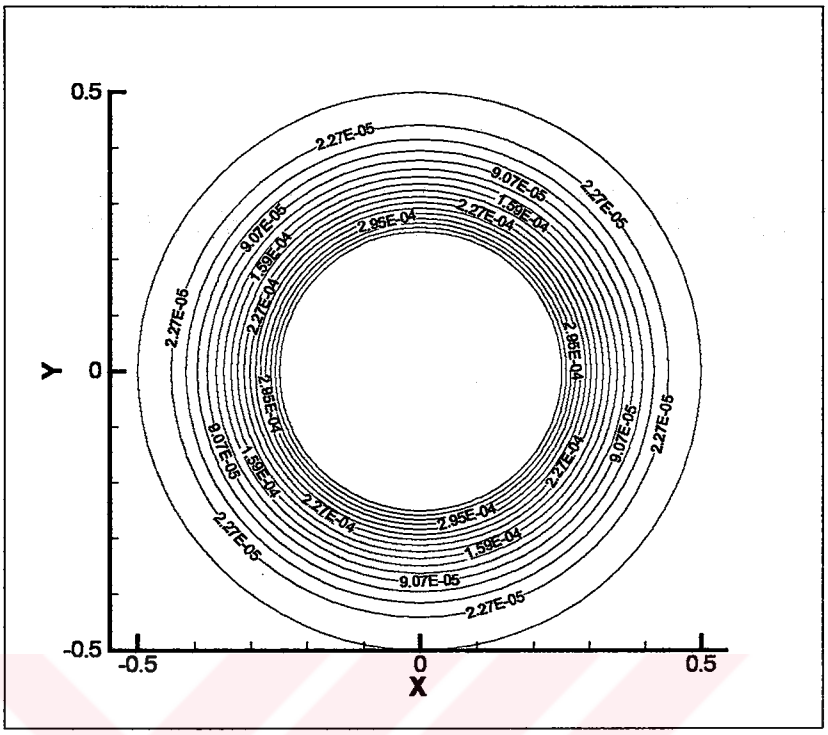

Figure 5.11 Streamline plot for case 11

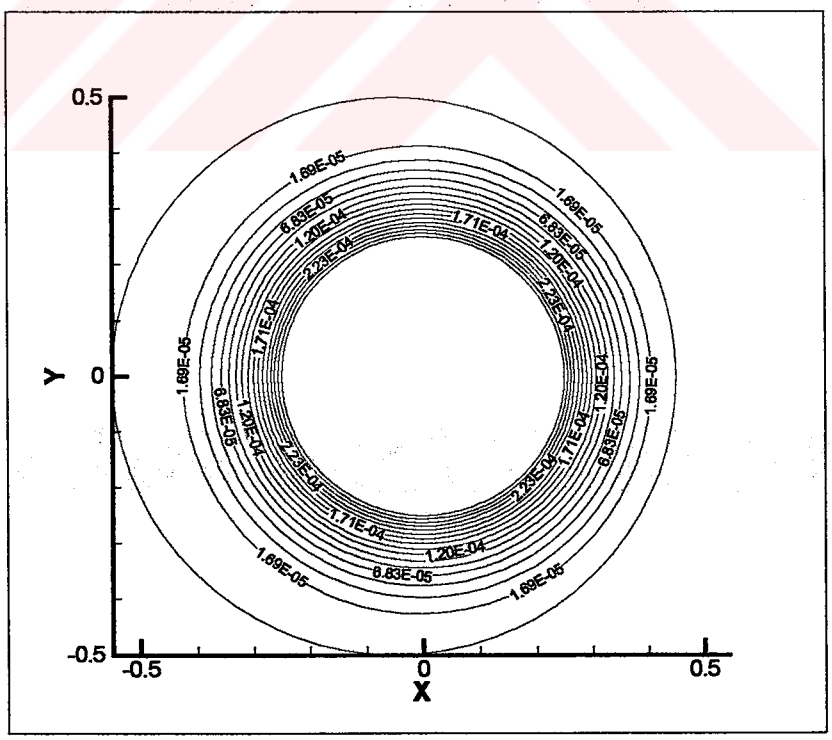

Figure 5.12 Streamline plot for case 12

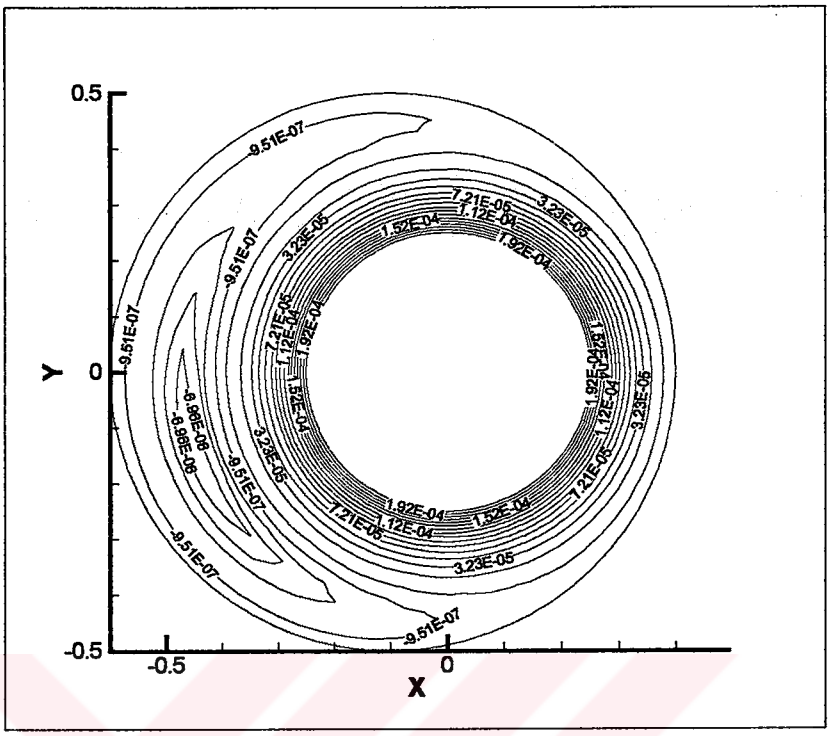

Figure 5.13 Streamline plot for case 13

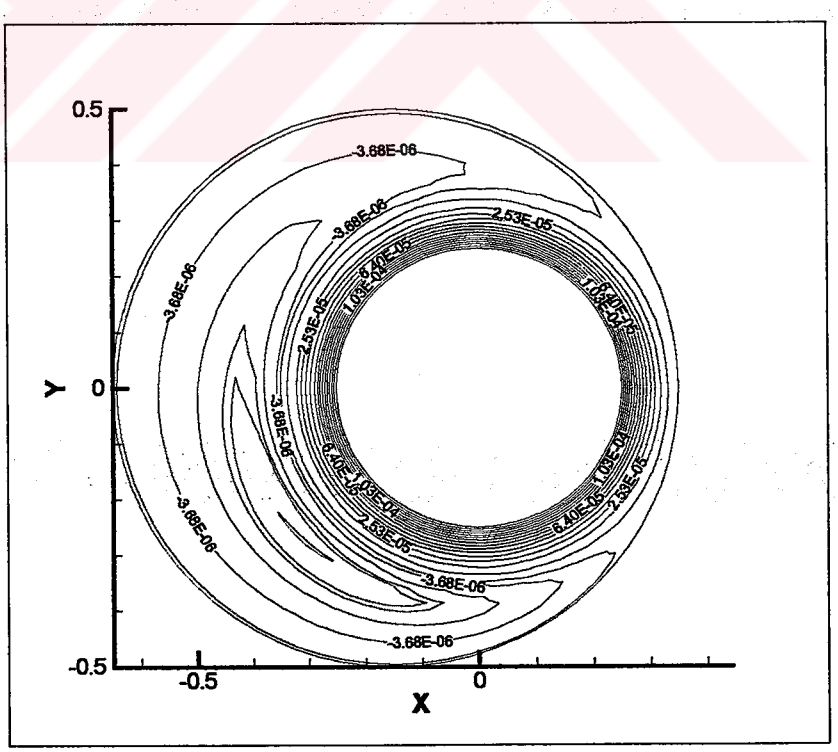

Figure 5.14 Streamline plot for case 14

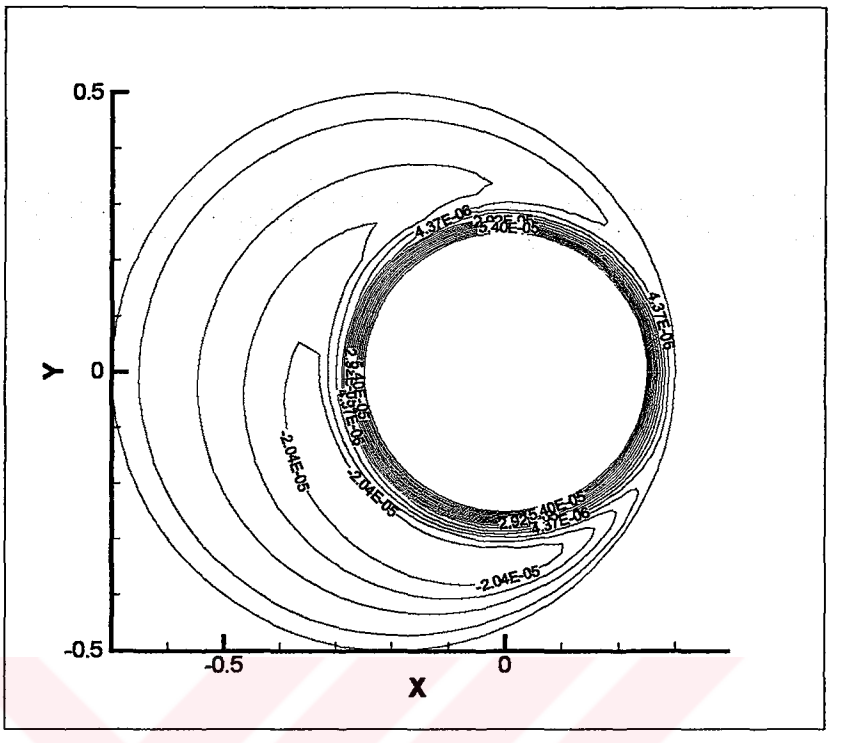

Figure 5.15 Streamline plot for case 15

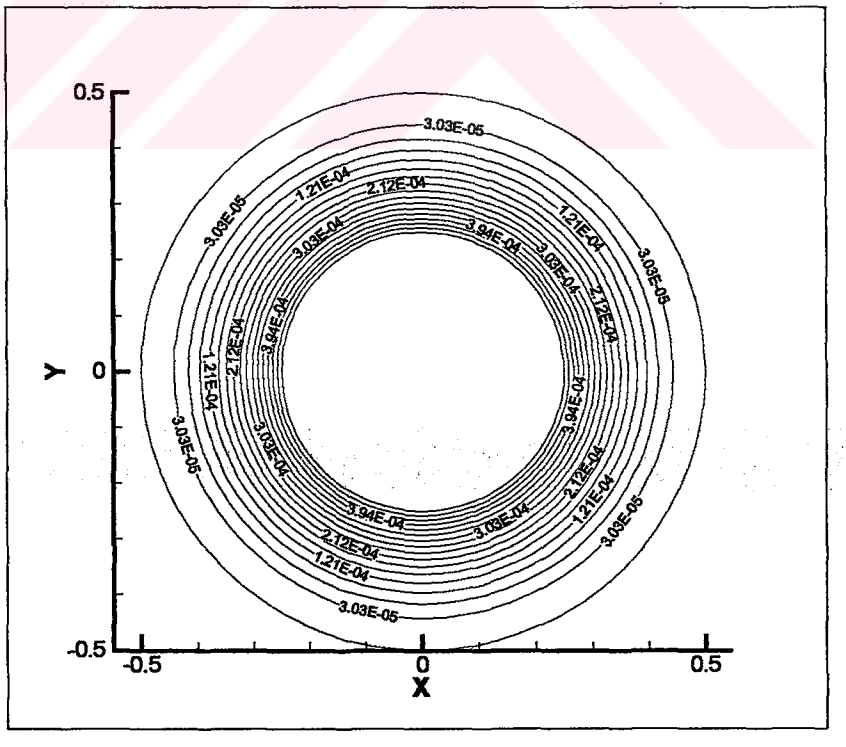

Figure 5.16 Streamline plot for case 16

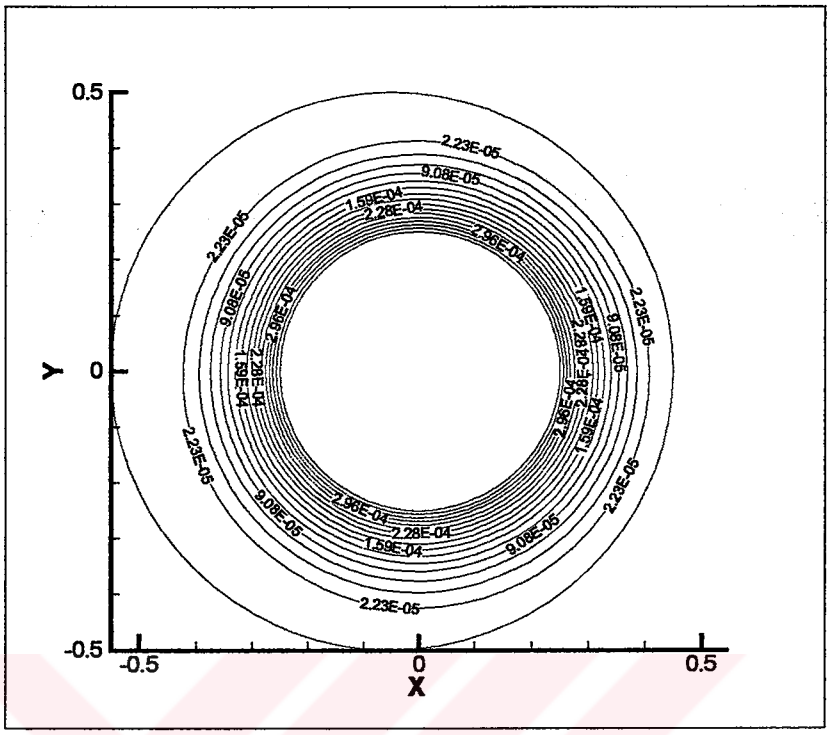

Figure 5.17 Streamline plot for case 17

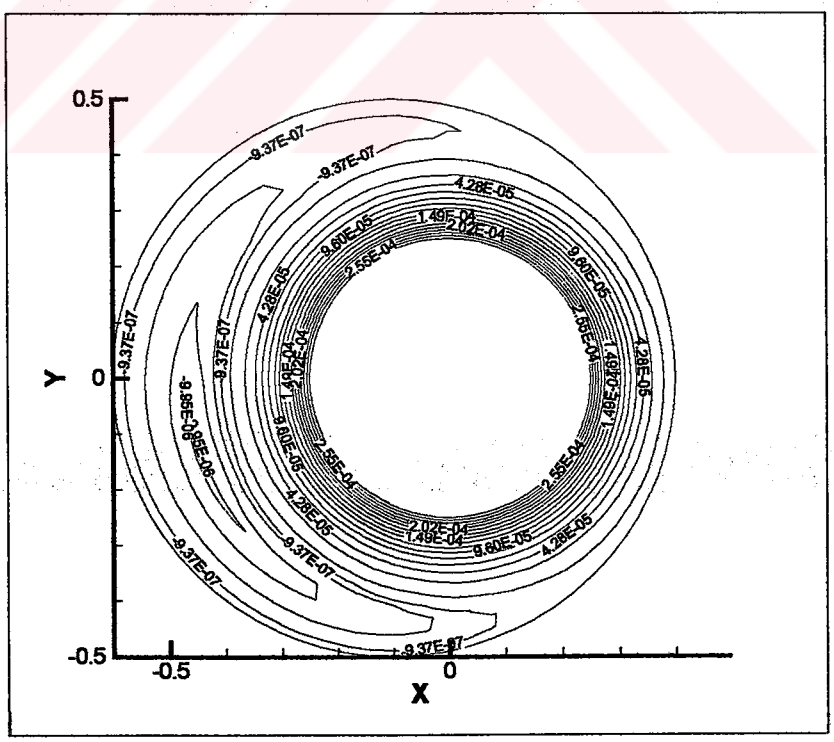

Figure 5.18 Streamline plot for case 18

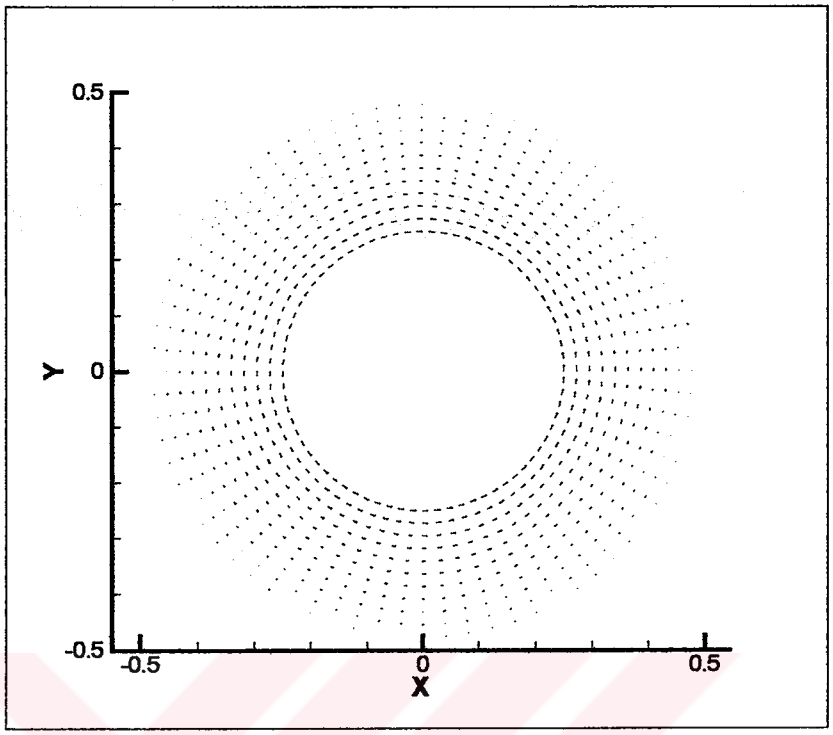

Figure 5.19 Vector plot of velocities for case 1

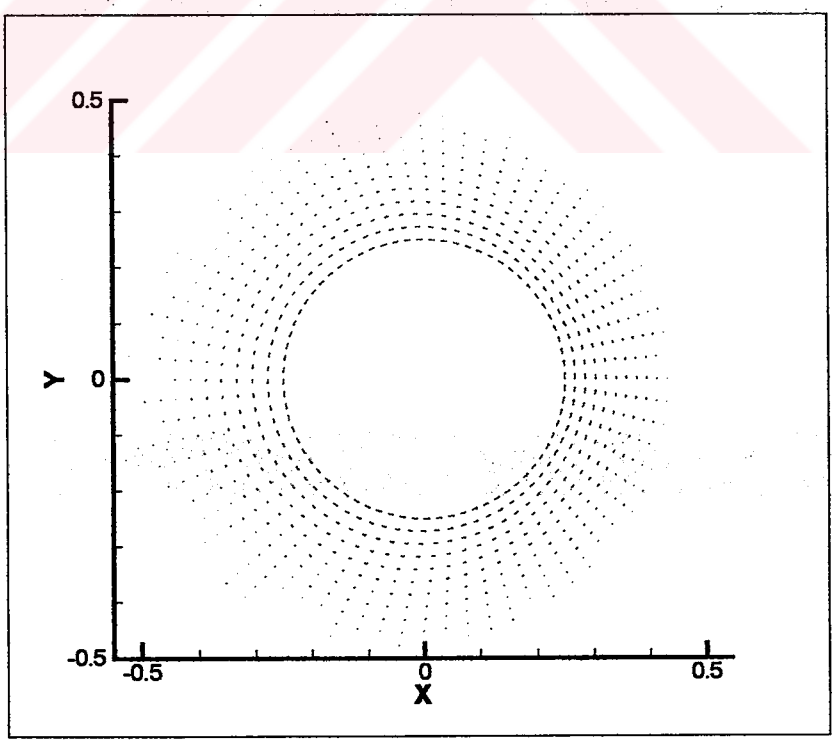

Figure 5.20 Vector plot of velocities for case 2

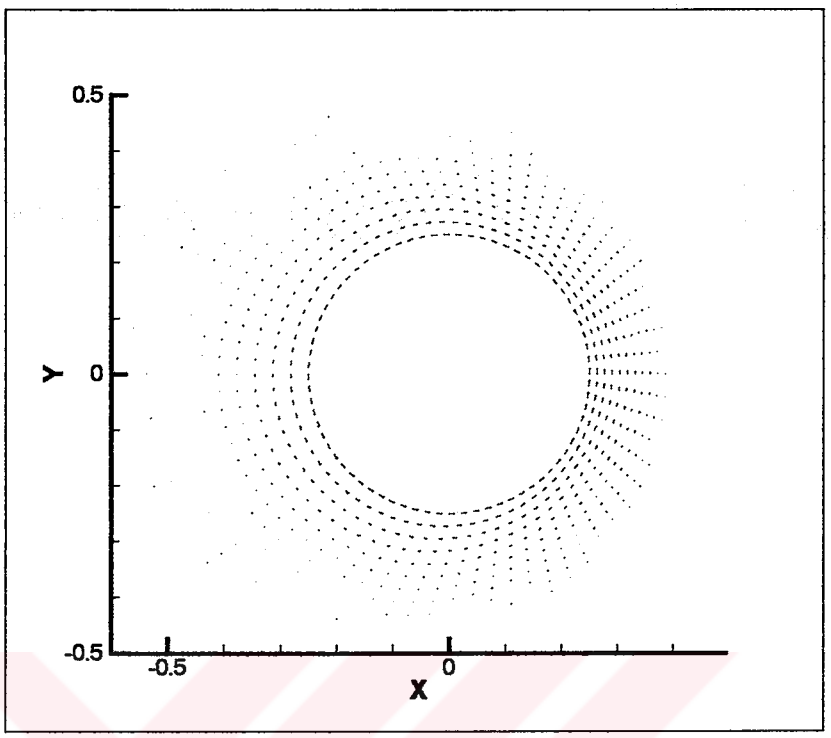

Figure 5.21 Vector plot of velocities for case 3

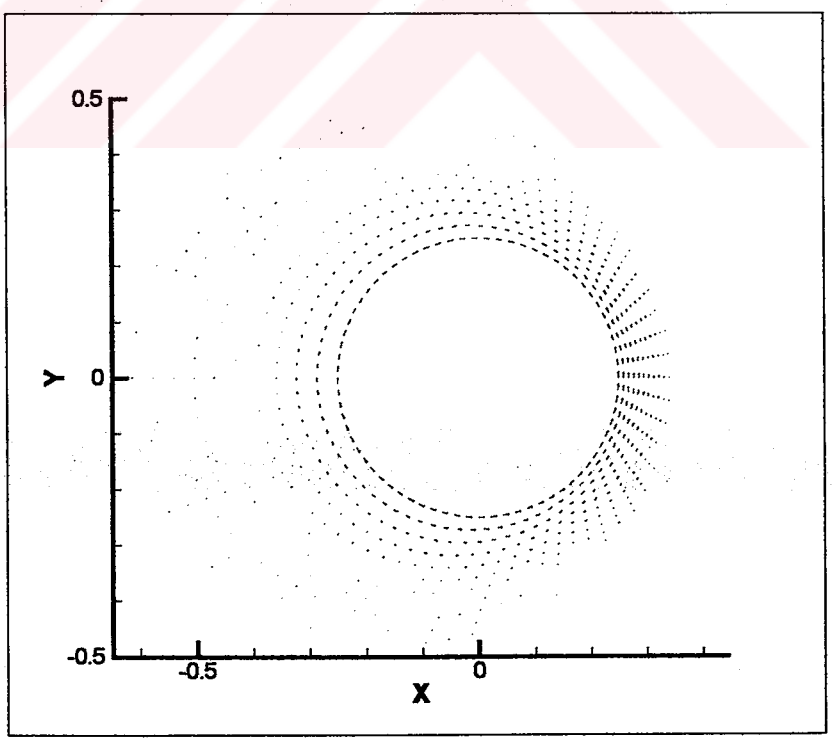

Figure 5.22 Vector plot of velocities for case 4

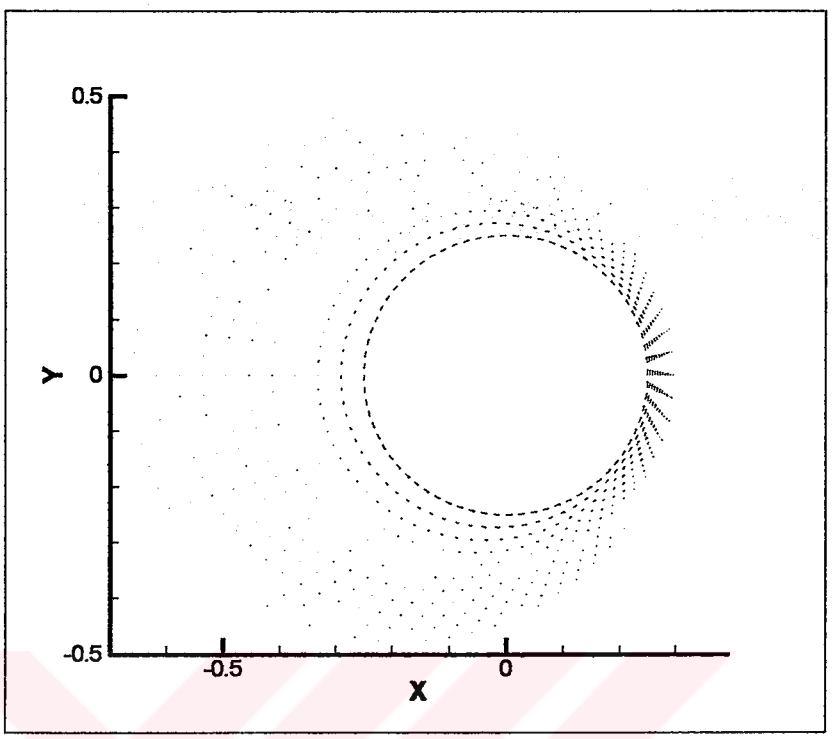

Figure 5.23 Vector plot of velocities for case 5

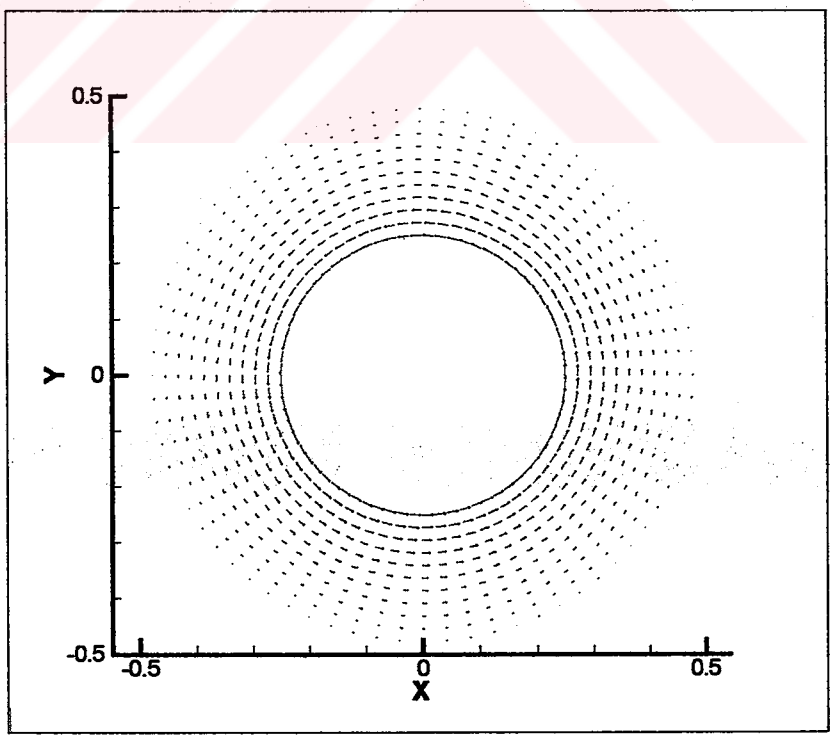

Figure 5.24 Vector plot of velocities for case 6

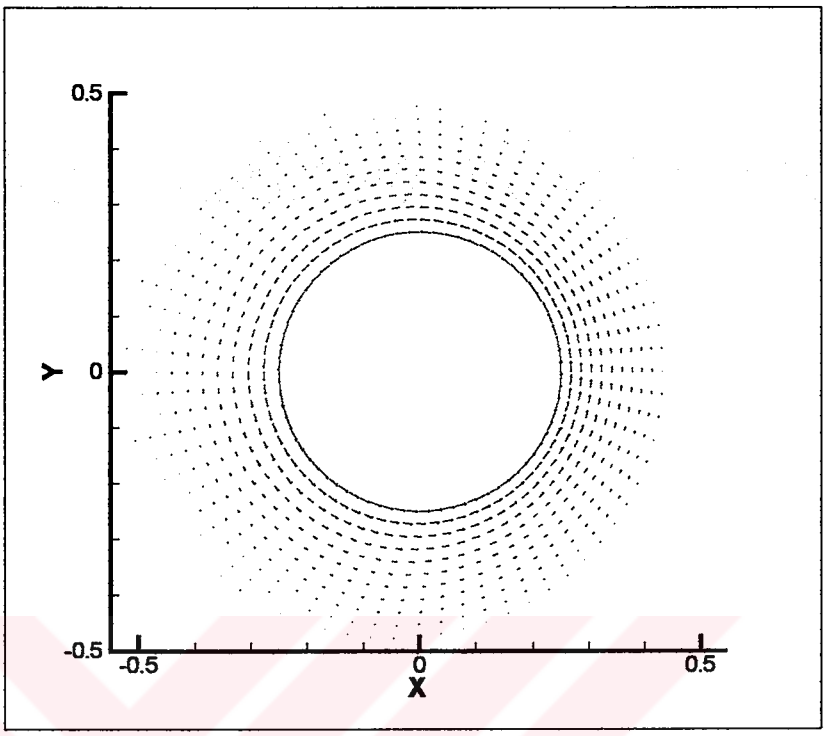

Figure 5.25 Vector plot of velocities for case 7

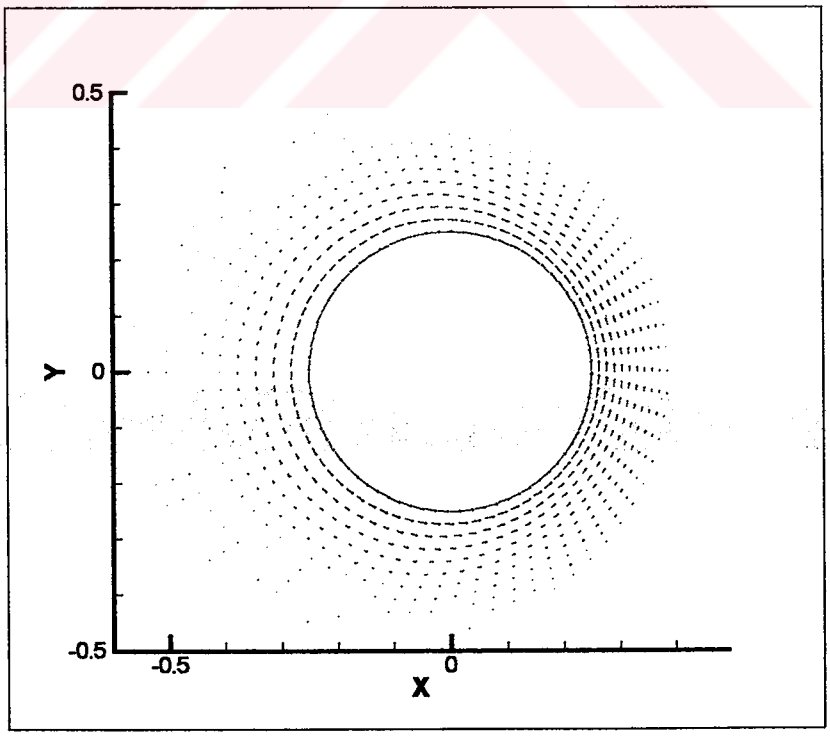

Figure 5.26 Vector plot of velocities for case 8

T.C. YÜKSEKÖĞRETİM KURULU
DOKÜMANTASYON MERKEZİ

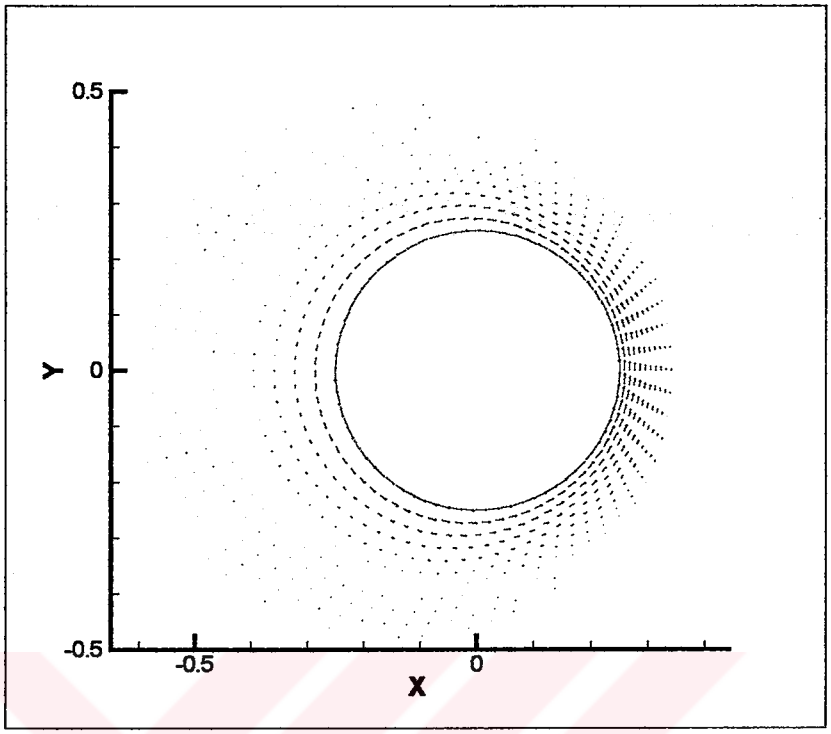

Figure 5.27 Vector plot of velocities for case 9

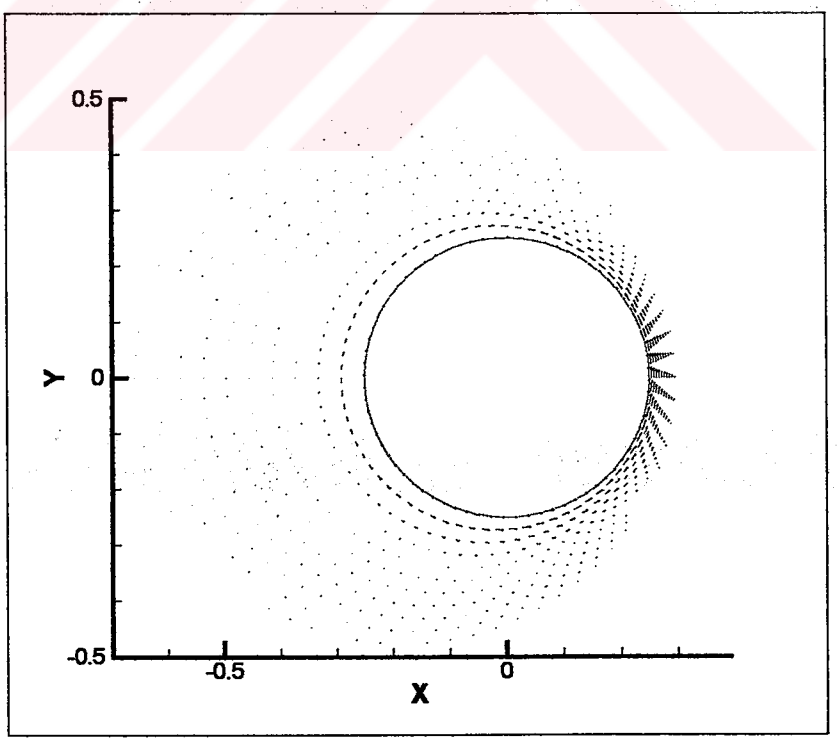

Figure 5.28 Vector plot of velocities for case 10

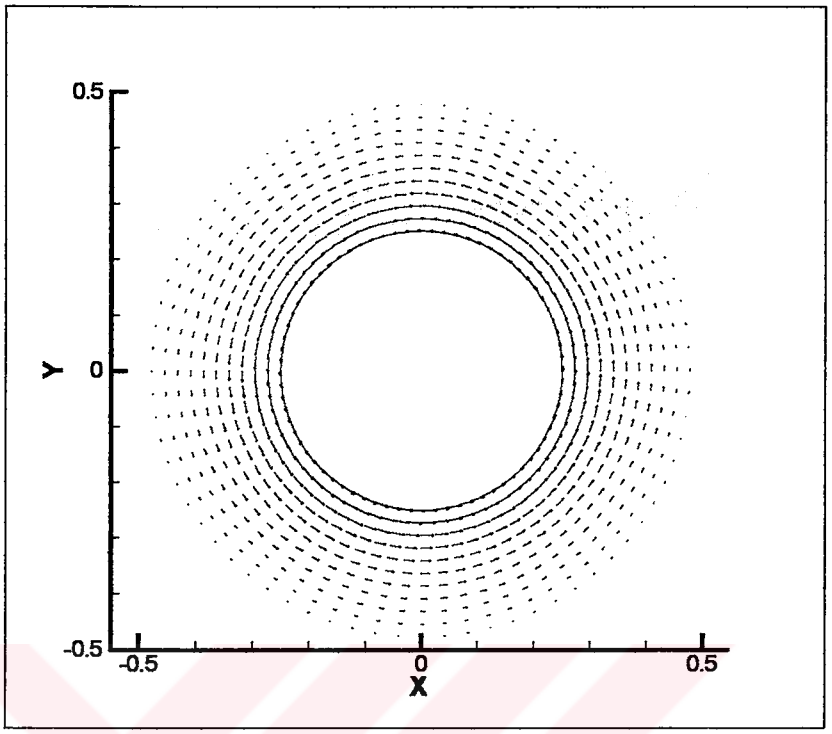

Figure 5.29 Vector plot of velocities for case 11

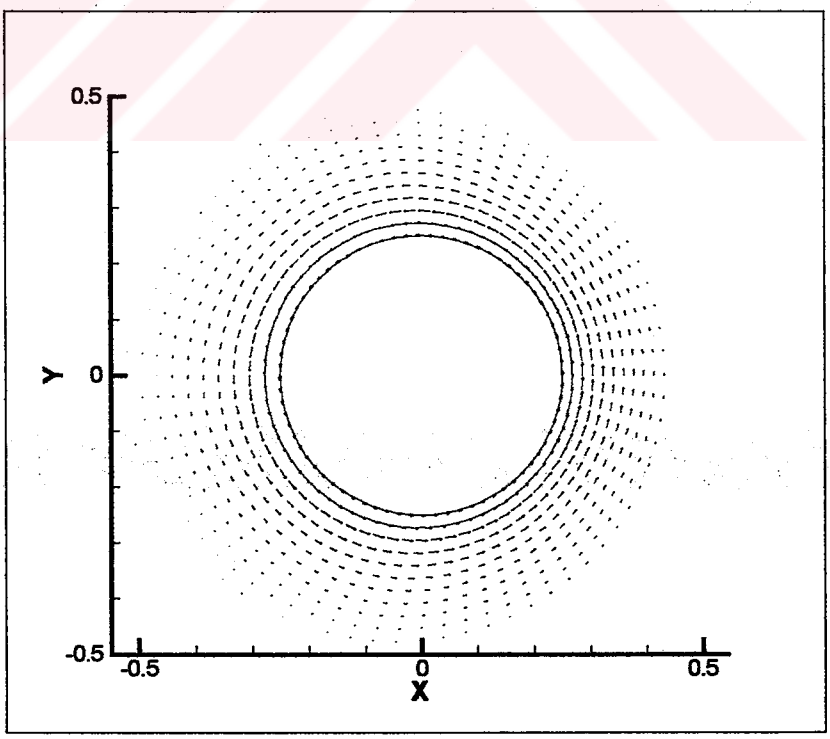

Figure 5.30 Vector plot of velocities for case 12

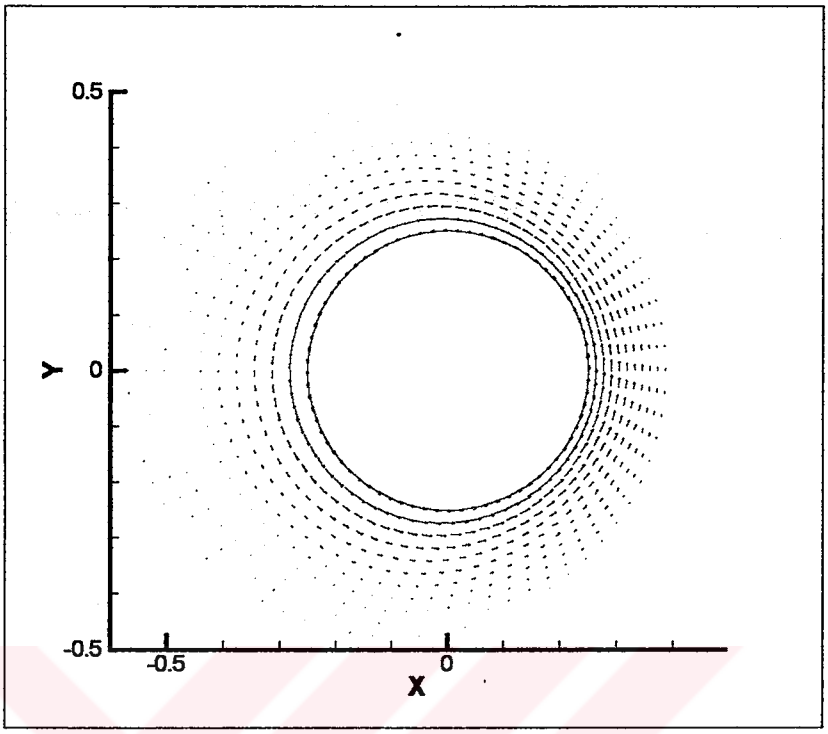

Figure 5.31 Vector plot of velocities for case 13

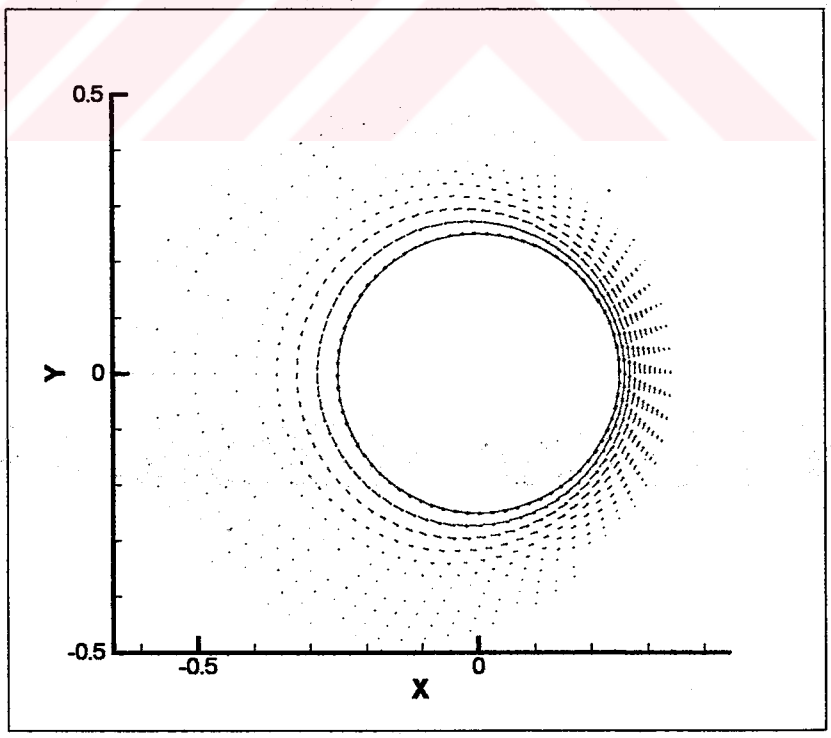

Figure 5.32 Vector plot of velocities for case 14

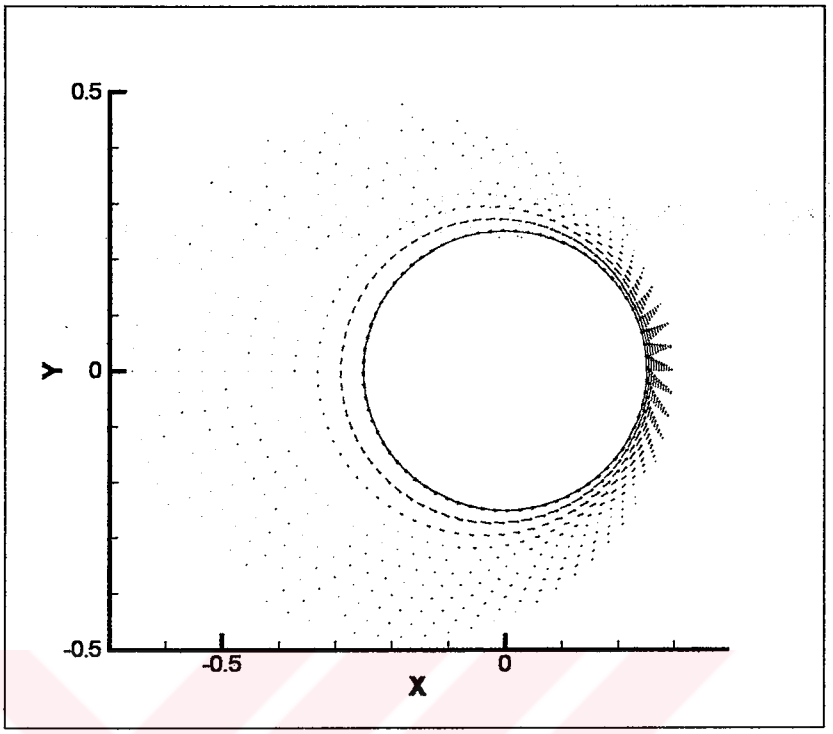

Figure 5.33 Vector plot of velocities for case 15

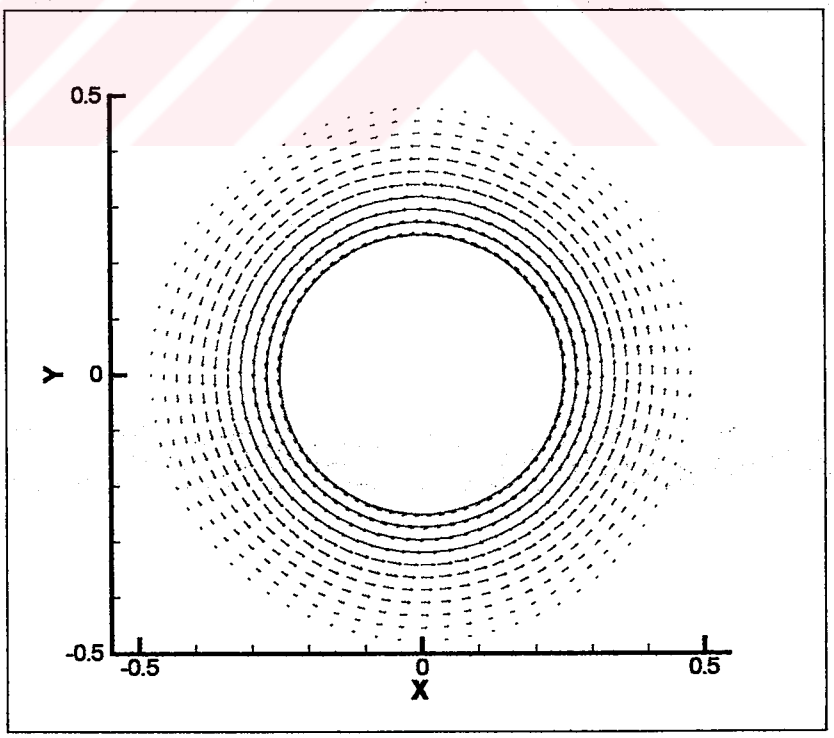

Figure 5.34 Vector plot of velocities for case 16

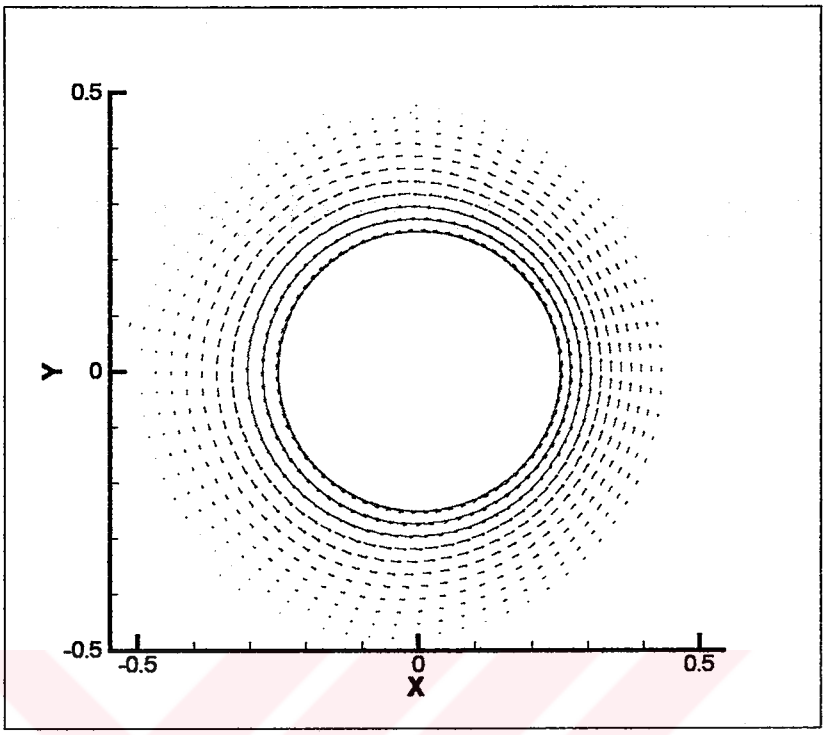

Figure 5.35 Vector plot of velocities for case 17

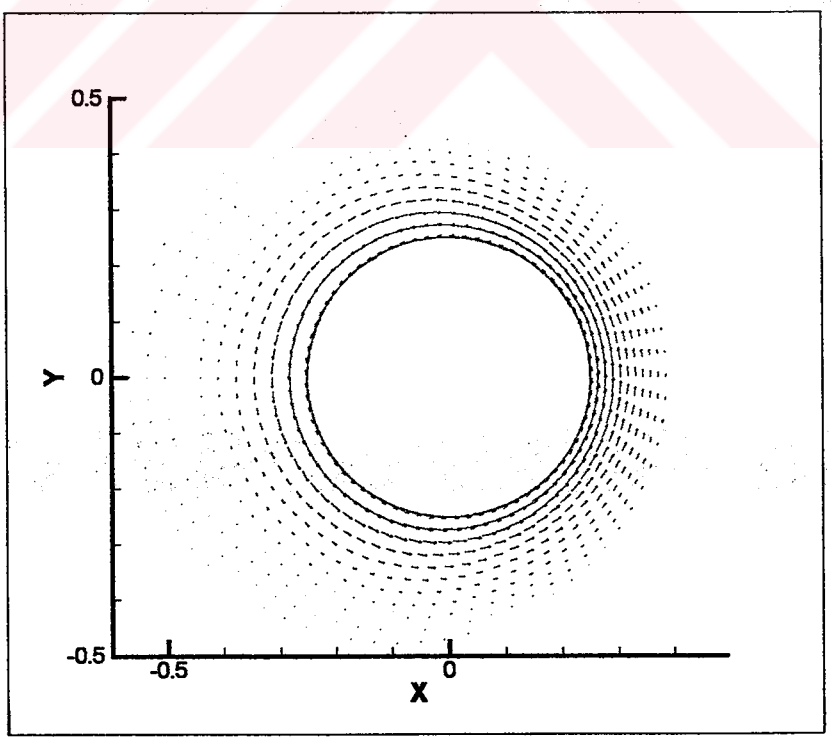

Figure 5.36 Vector plot of velocities for case 18

5.2 Discussion on the Results of Case Studies

Twenty case studies are carried out. Except for the cases 19 and 20 all cases converged to a solution. No special handling of convective terms is made in vorticity stream function formulation. It is seen that for caseS 19 and 20 both the Reynolds number is 1000 and eccentricity is at least 60%. High Reynolds numbers makes the equation to act like a convective equation, not a convective-diffusive equation. So special techniques such as upwinding should be applied to the convective terms.

It is seen that with the increase in eccentricity, Taylor vortices begun to appear. For low Reynolds numbers the velocities in widest part of the flow area are very small. When the rotation of the inner cylinder is high, that is the Reynolds number is high, the Taylor vortices dominate flow pattern. The velocities in this vortices increase with Reynolds number.

The computations are carried out on a time iteration basis. The effects of Reynolds number and eccentricity on the computational time are compared in figures 5.37 and 5.38. As the number of iterations increase, the CPU time also increases and even become cumbersome for a computer with Pentium4 1.6 GHz processor.

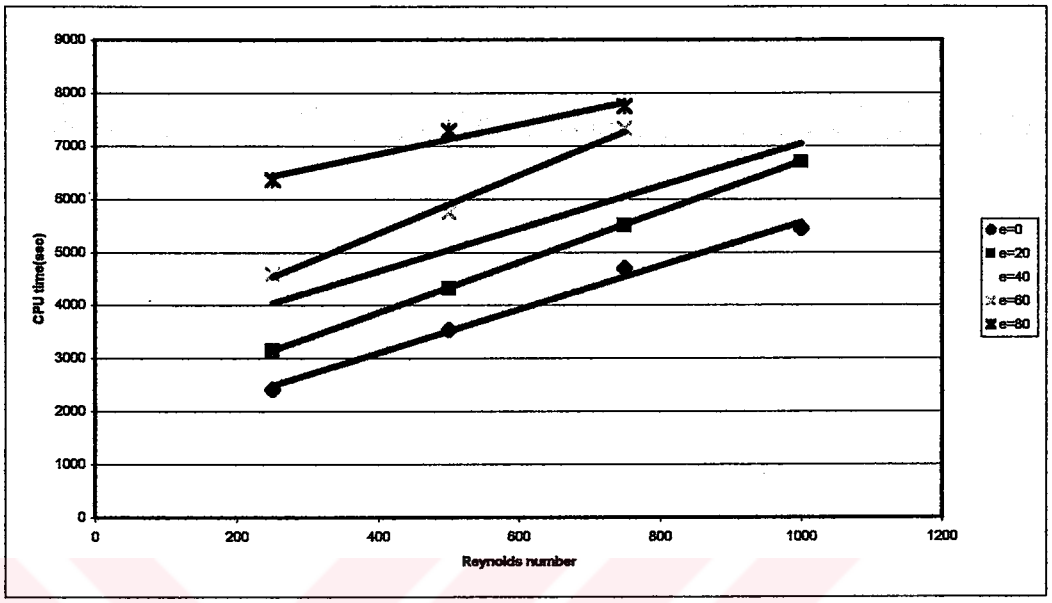

Figure 5.37 Effect of Reynolds number on CPU time

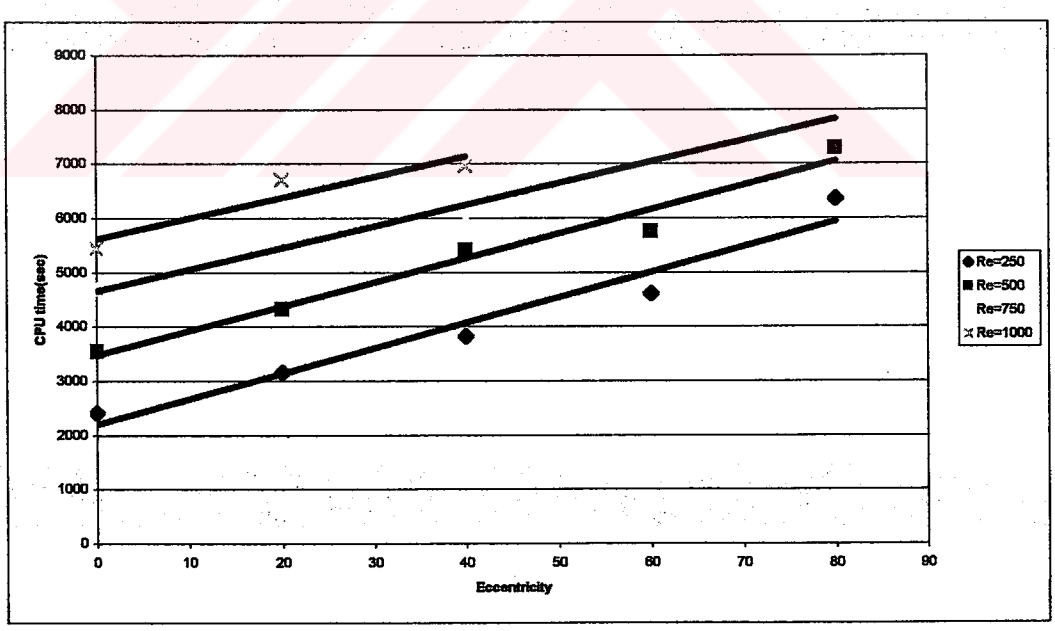

Figure 5.38 Effect of Eccentricity on CPU time

5.3 Validation of Results

At first, the numerical scheme employed, that is generalized finite difference method, is applied to the classical cavity problem to check the procedures. The findings that proved the validity of the procedures is given in Appendix B.

To check the validity of the results obtained for the problem at hand, the analytical solution of the governing equation for concentric case is used.

When the inner cylinder is rotating with an angular velocity of (ω_1) an the outer cylinder is stationary and the two cylinders are concentric, there exists an analytical solution to the Navier-Stokes equation. The radius ratio of outer cylinder to inner cylinder is 2. The governing equation in cylindrical coordinates becomes θ -component of Navier-Stokes equations due to concentricity. That is:

$$\frac{\partial v_\theta}{\partial t}+v_r\frac{\partial v_\theta}{\partial r}+\frac{v_\theta}{r}\frac{\partial v_\theta}{\partial \theta}+\frac{v_r v_\theta}{r}=-\frac{1}{\rho}\frac{\partial P}{\partial \theta}+\upsilon\left(\frac{\partial^2 v_\theta}{\partial r^2}+\frac{1}{r}\frac{\partial v_\theta}{\partial r}-\frac{v_\theta}{r^2}+\frac{1}{r^2}\frac{\partial^2 v_\theta}{\partial \theta^2}+\frac{2}{r^2}\frac{\partial v_r}{\partial \theta}\right) \tag{5.3}$$

where v_r is the velocity in radial direction which is zero because of the symmetry, v_θ is the velocity in angular direction, ρ is the density of the fluid and υ is the viscosity of the fluid. Furthermore, because of symmetry the $\frac{\partial}{\partial \theta}$ derivative is

also zero for any function. Taking into account that the flow is steady, The equation 5.3 reduces into the following form:

$$\frac{\partial^2 v_\theta}{\partial r^2}+\frac{1}{r}\frac{\partial v_\theta}{\partial r}-\frac{v_\theta}{r^2}=0 \tag{5.4}$$

A change of variable is needed in order to solve the equation.

Let

$$\varsigma = \ln r \tag{5.5}$$

then

$$\frac{\partial v_\theta}{\partial r}=\frac{\partial v_\theta}{\partial \varsigma}\frac{\partial \varsigma}{\partial r}=\frac{1}{r}\frac{\partial v_\theta}{\partial \varsigma} \tag{5.6}$$

and

$$\frac{\partial^2 v_\theta}{\partial r^2}=\frac{1}{r}\frac{\partial^2 v_\theta}{\partial \varsigma^2}\frac{\partial \varsigma}{\partial r}-\frac{1}{r^2}\frac{\partial v_\theta}{\partial \varsigma}=\frac{1}{r^2}\left(\frac{\partial^2 v_\theta}{\partial \varsigma^2}-\frac{\partial v_\theta}{\partial \varsigma}\right) \tag{5.7}$$

Inserting equation 5.6 and 5.7 into the equation 5.4 and making some simplification, it yields:

$$\frac{\partial^2 v_\theta}{\partial \varsigma^2}-v_\theta=0 \tag{5.8}$$

The solution to the above equation is of type:

$$v_\theta = Ae^{\varsigma} - Be^{-\varsigma} = Ar + \frac{B}{r} \tag{5.9}$$

The boundary conditions are no slip condition at the walls such that

$$v_\theta = \omega_1 R \text{ at } \quad r = R \tag{5.10}$$

$$v_\theta = 0 \text{ at } \quad r = 2R \tag{5.11}$$

Inserting the boundary conditions and solving for A and B yields

$$v_\theta = -\frac{1}{3}\omega_1 r + \frac{4}{3}\omega_1 \frac{R^2}{r} \tag{5.12}$$

The analytical solution is compared with that of the numerical results as depicted in figures 5.19 and 5.20.

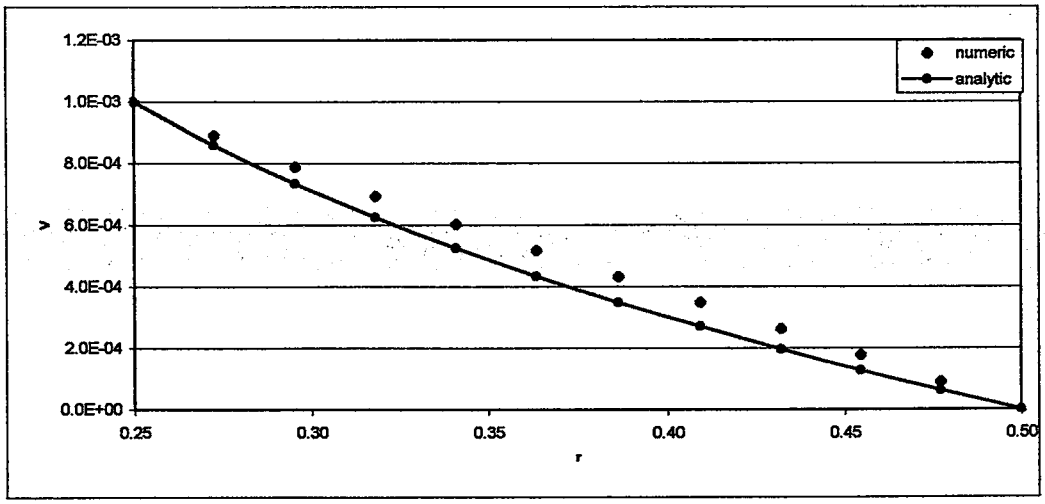

Figure 5.19 Comparison of Results with Analytical Solution for Re=250

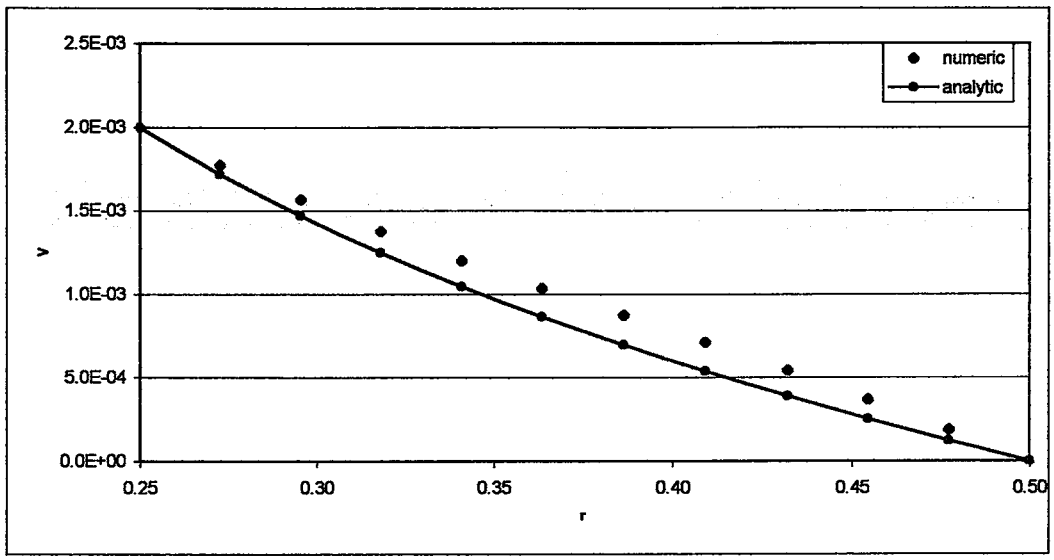

Figure 5.20 Comparison of Results with Analytical Solution for Re=500

As seen, the results are similar. A small deviation, approximately 5%, is seen for all Reynolds numbers. This shows that the discharge passing through the system is overestimated by the program.

5.4 Conclusion and Recommendations for Future Work

It has been shown that the generalized finite difference method can be used to handle complex flow phenomena with a success. However the implementation of the procedure, which may require the solution of large system of equation, may require a main frame.

Since majority of the experimental work on the subject, that is the flow between eccentric annuli, is in the turbulent regime, it is strongly recommended that

turbulence modeling must be coupled in to be able to check the validity of the prediction of the numerical procedure against the experimental findings.

Throughout this study, various primitive variables formulations were tried. It is understood that the pressure boundary conditions are the main problem for u-v-p formulation. To account for this a staggered grid should be used. Then no pressure boundary condition is needed. It is also seen that the convective terms can only be handled by an upwinding scheme. The method can be well integrated with finite volume strategy in order to be used with SIMPLE type solution techniques. It is then possible to study in 3-D problems for which the method will show its great capability.

The method is very efficient in handling the problems with complicated geometries and has high order approximations; but it has also some disadvantages. The memory and the time needed for the computations are higher than that of classical methods.

Despite its disadvantages, the method deserves to become more popular and widely used in near future because of its simplicity and flexibility in usage.

T.C. YÜKSEKÖĞRETİM KURULU
DOKÜMANTASYON MERKEZİ

REFERENCES

[1] Richard W. Johnson, "The Handbook of Fluid Dynamics," CRC Press 1998.

[2] İsmail Aydın, "Lecture Notes on Computational Fluid Dynamics," Civil Engineering Department,METU, February 2001.

[3] H. K. Versteeg, W. Malalasekera, " An introduction to Computational Fluid Dynamic," Longman,1995

[4] B.R. Munson, D.F. Young, T.H. Okiishi, "Fundamentals of Fluid Mechanics", John Wiley & Sons, 1998.

[5] S.C. Chapra, R.P. Canale, "Numerical Methods for Engineers," McGraw-Hill, 1998.

[6] R. Dai, Q. Dong, A. Z. Szeri, "Flow between eccentric rotating cylinders: Bifurcation and stability," International Journal of Engineering Science, Vol.30, No.10, pp.1323-1340, 1992.

[7] H. Usui, K. Tsuruta, "Analysis of fully developed turbulent flow in an eccentric annulus," Journal of Chemical Engineering of Japan, Vol.13, No.6, 1980.

[8] V. K. Jonsson, E. M. Sparrow, "Experiments on turbulent flow phenomena in eccentric annular ducts," Journal of Fluid Mechanics, Vol.25, Part I, pp. 65-86, 1966.

[9] W. T. Snyder, G. A. Goldstein, "An analysis of fully developed laminar flow in an eccentric annulus," A.I.Ch.E. Journal, Vol.11, No.3, pp.462-467, 1965.

[10] J. M. Nouri, H. Umur, J. H. Whitelaw, "Flow of newtonian and non-newtonian fluids in concentric and eccentric annuli," Journal of Fluid mechanics, Vol.253, pp. 617-641, 1993.

[11] L. N. Tao, W. F. Donovan, "Through-flow in concentric and eccentric annuli of fine clearance with and without relative motion of the boundaries," ASME paper, No. 54-A175, 1954.

[12] J. F. Heyda, "A Green's function solution for the case of laminar incompressible flow between non-concentric circular cylinders, "Journal of Franklin Institute, Vol. 267, pp. 25-34, 1959.

[13] C. A. Jones, "On flow between counter-rotating cylinders," Journal of fluid mechanics, Vol. 120, pp. 433-450, 1982.

[14] F.Badr, M. N. Farah, M. Badran, "A study on laminar motion of a viscous incompressible fluid between two parallel eccentric cylinders," Mechanics Research Communications, Vol 19. pp. 48,49, 1992.

[15] N. Gravas, B. W. Martin, "Instability of viscous axial flow in annuli having a rotating inner cylinder," Journal of fluid mechanics, Vol. 86, part 2, pp. 385-394, 1978.

[16] R. M. Lueptow, A. Docter, K. Min, "Stability of axial flow in an annulus with a rotating inner cylinder," Physics of fluids, A 4 (11), 1992.

[17] E. Kit, E. Mazor, "Numerical solution of laminar flow generated in an annulus by rotating screens," Acta Mechanica, Vol. 83, pp. 9-24, 1990.

[18] M. P. Escudier, P. J. Oliveira, F. T. Pinho, "Fully developed laminar flow of purely viscous non-Newtonian liquids through annuli, including the effects of eccentricity and inner-cylinder rotation," International Journal of Heat and Fluid Flow, Vol 23, pp. 52-73, 2002.

[19] M. Char, Y. Hsu, "Computation of buoyancy-driven flow in an eccentric centrifugal annulus with a non-orthogonal collocated finite volume algorithm," Journal for numerical methods in fluids, Vol. 26, pp. 323-343, 1998.

[20] M. Quadrio, P. Luchini, "Direct numerical simulation of the turbulent flow in a pipe with annular cross-section," European Journal of Mechanics B/Fluids, 2002.

[21] I. Raspo, S. Hugues, E. Serre, A. Randriamampianina, P. Bontoux, "A spectral projection method for the simulation of complex three-dimensional rotating flows," Computers and fluids, Vol.31, pp. 745-767, 2002.

[22] J. B. V. Wanderley, C. A. Levi, "Validation of a finite difference method for the simulation of vortex-induced vibrations on a circular cylinder," Ocean Engineering, Vol. 29, pp. 445-460, 2002.

[23] T. Liszka, J. Orkisz, "The finite difference method at arbitrary irregular grids and its application in applied mechanics," Computers and Structures, Vol. 11, pp 83-95,1980.

[24] Tadeusz Liszka, "An interpolation method for an irregular net of nodes," International Journal for Numerical Metehods in Engineering, Vol. 20 , pp. 1599-1612, 1984

[25] L. Gavate, J.L. Cuesta, "A numerical comparison of two different meshless methods," European Conference on Computational Mechanics, 2001.

[26] N. Perrone, R. Kao. " A general finite difference method for arbitrary meshes," Computers and Structures, Vol. 5, pp 45-58,1975.

[27] J.J. Benito, F. Urena, L. Gavate, " Influence of several factors in the generalized finite difference method," Applied Mathematical Modelling, Vol. 25, pp 1039-1053, 2001.

[28] J. Bonet, S. Kulasegaram, "A simplified approach to enhance the performance of smooth particle hydrodynamics methods," Applied Mathematics and Computation, Vol. 126, pp 133-155, 2002.

[29] D. Tang, C. Yang, S. Kobayashi, D.N. Ku, "Generalized finite difference method for 3-D viscous flow in stenotic tubes with large wall deformation and collapse," Applied Numerical Mathematics, Vol. 38, pp. 49-68, 2001.

[30] D. Tang, C. Yang, S. Kobayashi, D.N. Ku, "Experiment based numerical simulation of unsteady viscous flow in stenotic collapsible tubes," Applied Numerical Mathematics, Vol. 36, pp. 299-320, 2001.

[31] C. Shu, K.H.A. Wee, "Numerical simulation of natural convection in asquare cavity by SIMPLE-generalized differential quadrature method," Computers and Fluids, Vol. 31, pp 209-226,2002.

[32] N. Anders Petersson, "Stability of pressure boundary conditions for Stokes and Navier-Stokes equations," Journal of Computational Physics, Vol. 172, pp 40-70,2001.

[33] K. Amedodji, G. Bayada, M. Chambat, "On the unsteady Navier-Stokes equations in a time-moving domain with velocity-pressure boundary conditions," Nonlinear Analysis, Vol. 49, pp 565-587,2002.

[34] W. Layton, H.K. Lee, J. Peterson, "A defect-correction method for the incompressible Navier-Stokes equations," Applied Mathematics and Computation, Vol. 129, pp 1-19, 2002.

[35] T. Belytschko, D. Organ, Y. Krongauz, "A coupled finite element-element free Galerkin-method." Northwestern University, September 12,1995

[36] J.Dolbow, T. Belytschko, " An Introduction to programming the meshless element free Galerkin method," Northwestern University, July 3,1998

APPENDIX A

THE CODE OF THE COMPUTER PROGRAM

```
program mesh
USE numerical_libraries
implicit none
integer, PARAMETER :: n=12,teta=5,mz=n*360/teta,mz3=mz*3
real*8 x,y,Rout,Rin,ecc,delta1,delta2,pi,A(5,5),K(5,mz),nu,mu,err,err
1,err2,Pboun
real*8 alfa,e,Rvar,ro,omega1,omega2,Re,Eu,CP(5,mz),deltaU,deltaV
real*8 xp,urfP,urfV,disc,stream1,stream2,dmin,deltat,vmax
real*8,dimension(mz)::vectorU1,vectorUn,vectorV1,vectorVn,loadvor,loa
dstream,vor,stream
real*8,dimension(mz,mz)::coeffvor,coeffstream
real*8,dimension(mz)::sssx,sssy,w,U,V,Us,Vs,slnvor,slnstream,vectorU,
vectorV
real*8,dimension(mz,5,mz)::C
real*4 aaa,time,aa
integer noden,bno,icounter,kutay,k1,k2,II,NZ,bni(mz)
integer jteta,i,ionluk,info,j,jj

! parameters for fluid
alfa=1.0E-1
nu=1.0E-6
mu=1.0E-3
ro=999.0
write(*,*) 'node number=',mz

! input values
omega1=0.004
omega2=0.0
Rout=0.5
Rin=0.25
ecc=0.0
pi=3.14159265358979323846264338832
err=20

! Reynolds number
Re=max(abs(omega1*Rin*Rin/nu),abs(omega2*Rout*Rout/nu))
write (*,*) 'Re=',Re

delta1=Rout-ecc-Rin
delta2=Rout+ecc-Rin


!building the coordinates of the set of nodes

do 1002 jteta=0,360-teta,teta
```

```
do 1001 i=1,n
e=(delta2-delta1)*(i-1)/(n-1)/2
Rvar=(2*Rin+(delta1+delta2)*(i-1)/(n-1))/2
if (i.eq.1) then
bni(jteta*n/teta+i)=1
elseif(i.eq.2) then
bni(jteta*n/teta+i)=2
elseif(i.eq.(n-1)) then
bni(jteta*n/teta+i)=3
elseif(i.eq.n) then
bni(jteta*n/teta+i)=4
else
bni(jteta*n/teta+i)=0
endif
sssx(jteta*n/teta+i)=Rvar*cos(jteta*pi/180)-e
sssy(jteta*n/teta+i)=Rvar*sin(jteta*pi/180)
1001 continue


! velocity boundary conditions at walls (no slip)

U(jteta*n/teta+1)=-omega1*Rin*sin(jteta*pi/180)
V(jteta*n/teta+1)=omega1*Rin*cos(jteta*pi/180)
U(jteta*n/teta+n)=-omega2*Rout*sin(jteta*pi/180)
V(jteta*n/teta+n)=omega2*Rout*cos(jteta*pi/180)
1002 continue

dmin=min(Rin*teta*pi/180,delta1/n)
vmax=max(abs(omega1*Rin),abs(omega2*Rout))
deltat=dmin/(2.0*vmax)
write (*,*) 'timestep=',deltat


! building expressions for derivatives and storing them

aa=secnds(0.0)
icounter=0

do 1807 j=1,mz
    CP=0
call weigthfunction(K,A,sssx,sssy,j,mz,w,n,bni(j))
    call matrix_inversion (A,5)
    CP=matmul(A,K)
    do 1985 i=1,5
    do 1986 jj=1,mz
            C(j,i,jj)=CP(i,jj)
        1986 continue
    1985 continue
1807 continue
time=secnds(aa)
write (*,*) 'elapsed time for building=',time

!**********************************************************************
!**********************************************************************
!**********************************************************************
!**********************************************************************
!**********************************************************************

! begginnig to solve for the governing equations

do 1055 while (err.gt.1.0E-6)
icounter=icounter+1
```

```
disc=0.0
do 3278 i=2,n-1
disc=disc+V(i)
3278 continue

!calculating boundary conditions for stream function

stream1=delta1/(n-1)*((V(1)+V(n))/2.0+disc)
write (*,*) 'discharge=',stream1

! building equations for interior nodes


do 1008 ionluk=0,mz-n,n
do 1007 kutay=ionluk+2,ionluk+n-1
noden=kutay

do 1011 i=1,mz
    coeffvor(noden,i)=deltat*(U(noden)*C(noden,1,i)+V(noden)*C(noden,
2,i)-(C(noden,3,i)+C(noden,4,i))*nu)
    if (noden.eq.i) coeffvor(noden,i)=coeffvor(noden,i)+1
1011 continue
    loadvor(noden)=vor(noden)
1007 continue

! building equaitons for boundary nodes
    bno=ionluk

    coeffvor(bno+1,bno+1)=1
    coeffvor(bno+n,bno+n)=1

do 3579 i=1,mz
vectorU1(i)=-C(bno+1,2,i)*U(i)
vectorV1(i)=C(bno+1,1,i)*V(i)
vectorUn(i)=-C(bno+n,2,i)*U(i)
vectorVn(i)=C(bno+n,1,i)*V(i)
3579 continue

    loadvor(bno+1)=sum(vectorU1)+sum(vectorV1)
    loadvor(bno+n)=sum(vectorUn)+sum(vectorVn)
1008 continue

!solving the vorticity transport equation

call DLSARG(mz,coeffvor,mz,loadvor,1,slnvor)
vor=slnvor


! building equations for interior nodes

do 8008 ionluk=0,mz-n,n
do 8007 kutay=ionluk+2,ionluk+n-1
noden=kutay

do 8011 i=1,mz
    coeffstream(noden,i)=C(noden,3,i)+C(noden,4,i)
8011 continue

loadstream(noden)=-vor(noden)
8007 continue

! building equaitons for boundary nodes
```

```
coeffstream(ionluk+1,ionluk+1)=1
coeffstream(ionluk+n,ionluk+n)=1
loadstream(ionluk+1)=stream1
loadstream(ionluk+n)=0.0

8008 continue

!solving for the streamfunction values

call DLSARG(mz,coeffstream,mz,loadstream,1,slnstream)
stream=slnstream

Us=U
Vs=V

! calculating the velocity field

do 8638 ionluk=0,mz-n,n
do 8637 kutay=ionluk+2,ionluk+n-1
noden=kutay

do 6512 i=1,mz
vectorU(i)=C(noden,2,i)*stream(i)
vectorV(i)=-C(noden,1,i)*stream(i)
6512 continue
U(noden)=sum(vectorU)
V(noden)=sum(vectorV)

8637 continue
8638 continue

!calculating the error

err1=sum(abs(U-Us))/sum(abs(U))
err2=sum(abs(V-Vs))/sum(abs(V))
err=err1+err2
write (*,*) icounter,err

1055 continue

!writing results to an output file

k1=50000
open (k1,FILE='mesh.dat',STATUS='replace')
write (k1,*) 'VARIABLES=','"X",','"Y",','"U",','"V",','"Stream",'
write (k1,*) 'ZONE I=',n,',J=',mz/n+1,', F=POINT'
do 1003 i=1,mz+n
jj=i
if (i.gt.mz) jj=i-mz
1003 write (k1,1005) sssx(jj),sssy(jj),U(jj),V(jj),Stream(jj)
1005 format (1X,6E13.5)
1006 format (1X,4E7.2)
close (k1)

! writing properties of flow to an output file

k2=5000
time=secnds(aa)
write (*,*) 'total elapsed time =',time
write (*,*) 'reynold number=', Re, 'eccentricity=',ecc
```

```
open (k2,FILE='prop.txt',STATUS='replace')
write (k2,*) 'total time=',time
write (k2,*) 'reynold number=', Re
write (k2,*) 'eccentricity=',ecc
write (k2,*) 'number of nodes=',mz
write (k2,*) 'error=',err
write (k2,*) 'number of iterations=',icounter
write (k2,*) 'omega inner=',omega1
write (k2,*) 'omega outer=',omega2
close (k2)

stop
end


!**********************************************************************
!**********************************************************************
!**********************************************************************
!**********************************************************************
!**********************************************************************


subroutine weigthfunction (KK,A,X,Y,noden,numnode,ww,n,bni)
real*8,dimension(numnode):: X,Y,ww
real*8 Rin,A(5,5),KK(5,numnode),Uu,Vv
integer noden,numnode,n,bni
real*8 pwr
real*8,dimension(numnode)::k,h,h2,hk,h3,hk2,h2k,k2,k3,h4,h2k2,h3k,k4,
hk3,wh,wk,varkh,d,w
integer kt,wzero(numnode),south,southw,southe,souths,north,northw,nor
the,northn,east,easte,west,westw,mz
kt=noden
pwr=1.5
KK=0
A=0
mz=numnode

! selecting the nodes effecting the central node

if ((noden-n).lt.1) then
south=noden-n+mz
southw=noden-n-1+mz
southe=noden-n+1+mz
else
south=noden-n
southw=noden-n-1
southe=noden-n+1
endif

if ((noden+n).gt.mz) then
north=noden+n-mz
northw=noden+n-1-mz
northe=noden+n+1-mz
else
north=noden+n
northw=noden+n-1
northe=noden+n+1
endif
west=noden-1
westw=noden-2
east=noden+1
easte=noden+2
```

```
if((noden-n-n).lt.1) then
souths=noden-n-n+mz
else
souths=noden-n-n
endif
if((noden+n+n).gt.mz) then
northn=noden+n+n-mz
else
northn=noden+n+n
endif


wzero=0
if (bni.eq.0) then
wzero(north)=1
wzero(northw)=1
wzero(northe)=1
wzero(northn)=1
wzero(south)=1
wzero(southw)=1
wzero(southe)=1
wzero(souths)=1
wzero(west)=1
wzero(east)=1
wzero(westw)=1
wzero(easte)=1

elseif (bni.eq.1) then
wzero(north)=1
wzero(northe)=1
wzero(northn)=1
wzero(south)=1
wzero(southe)=1
wzero(souths)=1
wzero(east)=1
wzero(easte)=1

elseif (bni.eq.2) then
wzero(north)=1
wzero(northw)=1
wzero(northe)=1
wzero(northn)=1
wzero(south)=1
wzero(southw)=1
wzero(southe)=1
wzero(souths)=1
wzero(west)=1
wzero(east)=1
wzero(easte)=1


elseif (bni.eq.3) then
wzero(north)=1
wzero(northw)=1
wzero(northe)=1
wzero(northn)=1
wzero(south)=1
wzero(southw)=1
wzero(southe)=1
wzero(souths)=1
wzero(west)=1
wzero(east)=1
```

```
wzero(westw)=1


elseif (bni.eq.4) then
wzero(north)=1
wzero(northw)=1
wzero(northn)=1
wzero(south)=1
wzero(southw)=1
wzero(souths)=1
wzero(west)=1
wzero(westw)=1
endif


! calculating the weigths of the nodes effecting the central node
do 2001 i=1,numnode
h(i)=X(i)-X(noden)
k(i)=Y(i)-Y(noden)

if (i.eq.kt) then
w(i)=0
else
w(i)=(1.0/(h(i)**2.0+k(i)**2.0))**pwr
endif
2001 continue

w=w*wzero


do 3046 i=1,numnode
wh(i)=w(i)*w(i)*h(i)
wk(i)=w(i)*w(i)*k(i)
h2(i)=w(i)*w(i)*h(i)*h(i)
hk(i)=w(i)*w(i)*h(i)*k(i)
h3(i)=w(i)*w(i)*h(i)*h(i)*h(i)
hk2(i)=w(i)*w(i)*h(i)*k(i)*k(i)
h2k(i)=w(i)*w(i)*h(i)*h(i)*k(i)
k2(i)=w(i)*w(i)*k(i)*k(i)
k3(i)=w(i)*w(i)*k(i)*k(i)*k(i)
h4(i)=w(i)*w(i)*h(i)*h(i)*h(i)*h(i)
h2k2(i)=w(i)*w(i)*h(i)*h(i)*k(i)*k(i)
h3k(i)=w(i)*w(i)*h(i)*h(i)*h(i)*k(i)
k4(i)=w(i)*w(i)*k(i)*k(i)*k(i)*k(i)
hk3(i)=w(i)*w(i)*h(i)*k(i)*k(i)*k(i)

3046 continue

! building the derivative expressions

A(1,1)=sum(h2)
A(1,2)=sum(hk)
A(1,3)=sum(h3)/2
A(1,4)=sum(hk2)/2
A(1,5)=sum(h2k)
A(2,1)=A(1,2)
A(2,2)=sum(k2)
A(2,3)=sum(h2k)/2
A(2,4)=sum(k3)/2
A(2,5)=sum(hk2)
A(3,1)=A(1,3)
A(3,2)=A(2,3)
```

```
A(3,3)=sum(h4)/4
A(3,4)=sum(h2k2)/4
A(3,5)=sum(h3k)/2
A(4,1)=A(1,4)
A(4,2)=A(2,4)
A(4,3)=A(3,4)
A(4,4)=sum(k4)/4
A(4,5)=sum(hk3)/2
A(5,1)=A(1,5)
A(5,2)=A(2,5)
A(5,3)=A(3,5)
A(5,4)=A(4,5)
A(5,5)=sum(h2k2)

!generation of martix K

do 2006 i=1,5
    do 2007 j=1,numnode
        if (i.eq.1) then
        varkh=wh
        elseif (i.eq.2) then
        varkh=wk
        elseif (i.eq.3) then
        varkh=h2/2
        elseif (i.eq.4) then
        varkh=k2/2
        elseif (i.eq.5) then
        varkh=hk
        endif
        if (j.eq.noden) then
        KK(i,j)=-sum(varkh)
        else
        KK(i,j)=varkh(j)
        endif
    2007 continue
2006 continue

return
end


!**********************************************************************
!**********************************************************************
!**********************************************************************
!**********************************************************************
!**********************************************************************
      subroutine matrix_inversion ( A, NP )
      !-------------------------------------------------------------
      !
      !    Taken from "Numeric recipes".  The original program was
      !    GAUSSJ which solves linear equations by the Gauss_Jordon
      !    elimination method.  Only the parts required to invert
      !    matrices have been retained.
      !
      !    J.P. Griffith  6/88
      !
      !-------------------------------------------------------------

      PARAMETER (NMAX=50)
      Real*8    A(NP,NP)
      DIMENSION IPIV(NMAX), INDXR(NMAX), INDXC(NMAX)
```

```
      n = np

      DO 3011 J=1,N
        IPIV(J)=0
3011    CONTINUE
      DO 3022 I=1,N
        BIG=0.
        DO 3013 J=1,N
          IF(IPIV(J).NE.1)THEN
            DO 3012 K=1,N
              IF (IPIV(K).EQ.0) THEN
                IF (ABS(A(J,K)).GE.BIG)THEN
                  BIG=ABS(A(J,K))
                  IROW=J
                  ICOL=K
                ENDIF
              ELSE IF (IPIV(K).GT.1) THEN
                PAUSE 'Singular matrix'
              ENDIF
3012          CONTINUE
          ENDIF
3013      CONTINUE

        IPIV(ICOL)=IPIV(ICOL)+1
        IF (IROW.NE.ICOL) THEN
          DO 3014 L=1,N
            DUM=A(IROW,L)
            A(IROW,L)=A(ICOL,L)
            A(ICOL,L)=DUM
3014        CONTINUE
        ENDIF
        INDXR(I)=IROW
        INDXC(I)=ICOL
        IF (A(ICOL,ICOL).EQ.0.) PAUSE 'Singular matrix.'
        PIVINV=1./A(ICOL,ICOL)
        A(ICOL,ICOL)=1.
        DO 3016 L=1,N
          A(ICOL,L)=A(ICOL,L)*PIVINV
3016      CONTINUE
        DO 3021 LL=1,N
          IF(LL.NE.ICOL)THEN
            DUM=A(LL,ICOL)
            A(LL,ICOL)=0.
            DO 3018 L=1,N
              A(LL,L)=A(LL,L)-A(ICOL,L)*DUM
3018          CONTINUE
          ENDIF
3021      CONTINUE
3022    CONTINUE
      DO 3024 L=N,1,-1
        IF(INDXR(L).NE.INDXC(L))THEN
          DO 3023 K=1,N
            DUM=A(K,INDXR(L))
            A(K,INDXR(L))=A(K,INDXC(L))
            A(K,INDXC(L))=DUM
3023        CONTINUE
        ENDIF
3024    CONTINUE
      RETURN
      END
```

APPENDIX B

DRIVEN CAVITY FLOW

Another computer program is written for driven cavity flow in order to validate the results of the computer program for another type of problem, which is driven cavity flow problem.

An incompressible fluid is placed on a 2-D square cavity as shown in Figure B.1. The plate on the upper face is moved horizontally at a constant speed U_p. The laminar flow obtained by the moving plate is calculated using a vorticity stream function formulation by the meshless method. Also the problem is solved by finite difference method writing a computer code. The finite difference method and meshless method solutions are compared to validate the results of the meshless method.

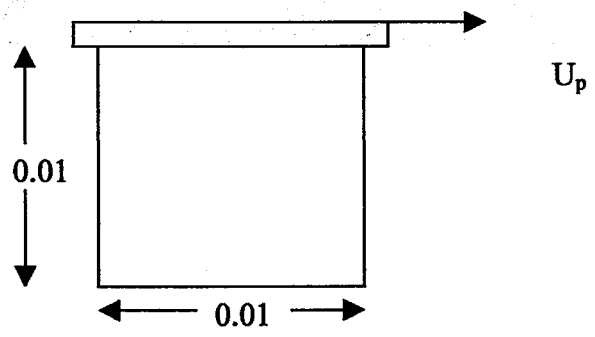

Figure B.1 An incompressible fluid placed on a 2-D square cavity

T.C. YÜKSEKÖĞRETİM KURULU
DOKÜMANTASYON MERKEZİ

The equation defining the flow is given by equations 4.1 and 4.5 similar to that of annular flow.

The alternating direction implicit method with first order upwind differences is used for the finite difference method.

The main difference in two programs is using first order upwind differences to handle the convective terms in vorticity transport equation in finite difference method solution. The finite difference solutions both with and without upwinding technique are given for comparison. No special technique like upwinding is applied to the convective terms in meshless method.

The same boundary conditions are used to calculate the boundary conditions for vorticity in both of the programs. These are the conditions given in equation 4.2. For the solution of the stream function values, equation 4.5 is solved in the domain with the vorticity values found from the solution of the vorticity transport equation.

The boundary conditions for the stream function are given as $\psi = 0$ for all solid boundaries since the boundaries themselves form a stream function. The streamlines are drawn and given in figures B.2 and B.3 for finite difference and meshless solutions, respectively.

The computer program with finite difference solution uses 50x50 meshes, whereas the program with meshless method uses 30x30 meshes due to computer limitations.

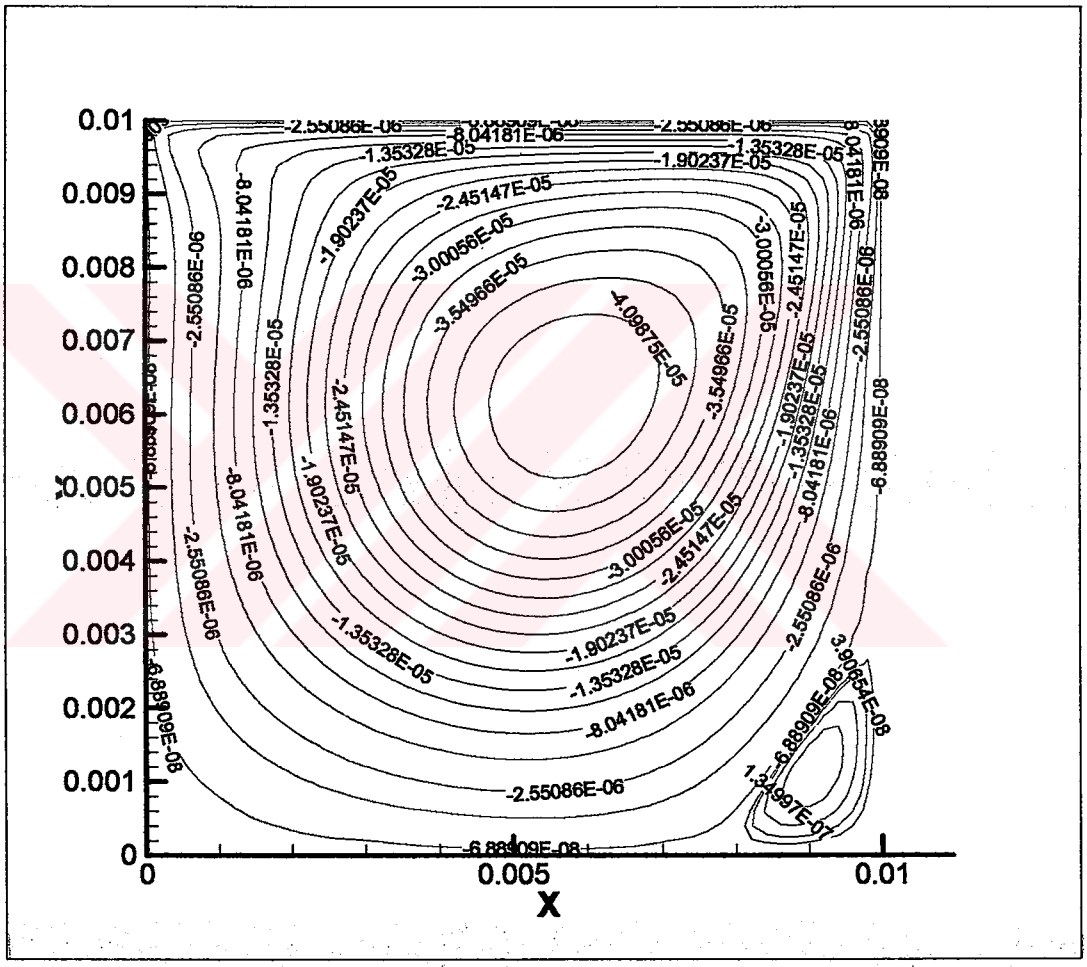

Figure B.2 Finite difference solution with upwinding

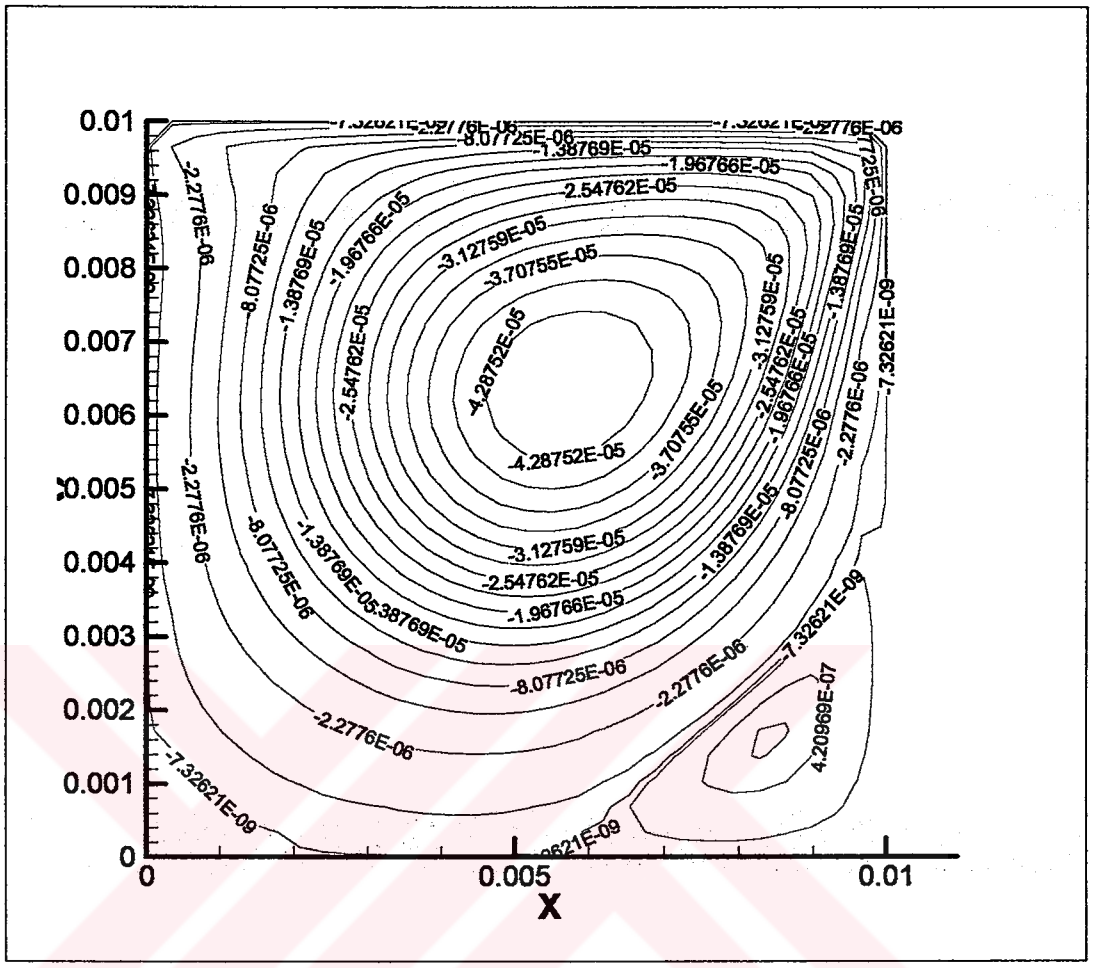

Figure B.3 Generalised finite difference (meshless) solution

The results of Driven Cavity Problem with finite difference formulation with upwinding can be compared to the results with meshless method, by comparing the maximum values of stream functions. For the finite difference solution with upwinding scheme, maximum stream function value is 4.373 E-5 whereas for the meshless method, the maximum stream function value is 4.577 E-5. Without upwinding , the finite difference solution gives a maximum stream function value of 5.559 E-5 (Figure B.4). The results of meshless solution seem to be much nearer to the finite difference solution with upwinding scheme.

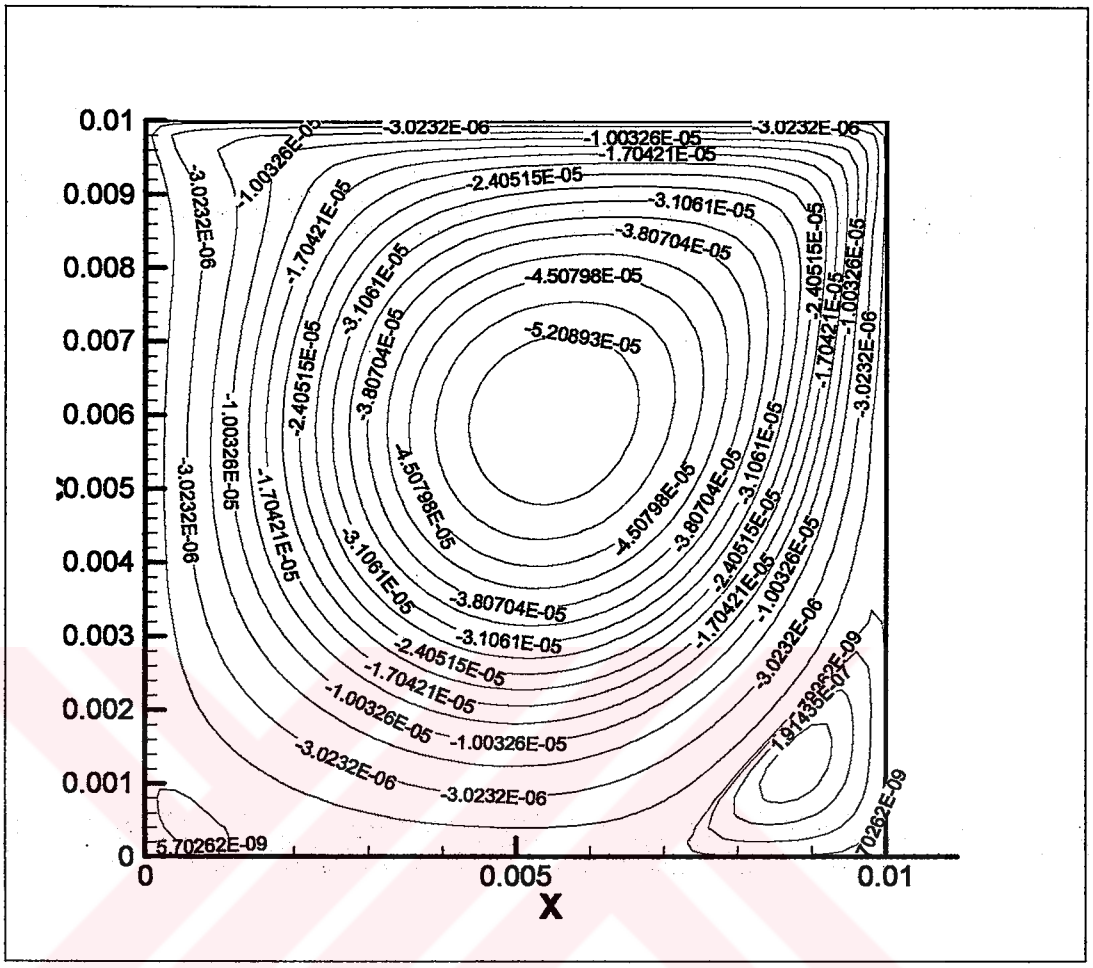

Figure B.4 Finite difference solution without upwinding

It is seen that the two standard finite difference solutions show different flow fields. This is because the upwinding technique somewhat smoothens the flow field. The meshless method gives a result in between these two standard finite difference methods.

T.C. YÜKSEKÖĞRETİM KURULU
DOKÜMANTASYON MERKEZİ